

8-7-2010

**Role of organic matter in formation of stromatolites and micritic ooids from Channing Lake Basin: Rita Blanca Formation; Panhandle, Texas**

Brittany Leigh Weeks

Follow this and additional works at: <https://scholarsjunction.msstate.edu/td>

---

**Recommended Citation**

Weeks, Brittany Leigh, "Role of organic matter in formation of stromatolites and micritic ooids from Channing Lake Basin: Rita Blanca Formation; Panhandle, Texas" (2010). *Theses and Dissertations*. 3834. <https://scholarsjunction.msstate.edu/td/3834>

This Graduate Thesis - Open Access is brought to you for free and open access by the Theses and Dissertations at Scholars Junction. It has been accepted for inclusion in Theses and Dissertations by an authorized administrator of Scholars Junction. For more information, please contact [scholcomm@msstate.libanswers.com](mailto:scholcomm@msstate.libanswers.com).

ROLE OF ORGANIC MATTER IN FORMATION OF STROMATOLITES AND  
MICRITIC OIDS FROM CHANNING LAKE BASIN; RITA BLANCA  
FORMATION; PANHANDLE, TEXAS

By

Brittany Leigh Weeks

A Thesis  
Submitted to the Faculty of  
Mississippi State University  
in Partial Fulfillment of the Requirements  
for the Degree of Masters of Science  
in Geosciences  
in the Department of Geosciences

Mississippi State, Mississippi

August 2010

Copyright 2010

By

Brittany Leigh Weeks

ROLE OF ORGANIC MATTER IN FORMATION OF STROMATOLITES AND  
MICRITIC OIDS FROM CHANNING LAKE BASIN; RITA BLANCA  
FORMATION; PANHANDLE, TEXAS

By

Brittany Leigh Weeks

Approved:

---

Brenda L. Kirkland  
Associate Professor of Geosciences  
Committee Chair

---

Chris P. Dewey  
Graduate Coordinator of Geosciences  
Committee Member

---

Darrel W. Schmitz  
Department Head of Geosciences  
Committee Member

---

Gary L. Myers  
Dean of College of Arts and Sciences

Name: Brittany Leigh Weeks

Date of Degree: August 7, 2010

Institution: Mississippi State University

Major Field: Geosciences

Major Professor: Brenda L. Kirkland

Title of Study: ROLE OF ORGANIC MATTER IN FORMATION OF  
STROMATOLITES AND MICRITIC OIDS FROM CHANNING  
LAKE BASIN; RITA BLANCA FORMATION; PANHANDLE,  
TEXAS

Pages in Study: 67

Candidate for Degree of Masters of Science

Channing Lake Basin, located west and northwest of Channing, in the Texas Panhandle, is of substantial area and presumably includes lake beds of Pliocene and Pleistocene ages within the Rita Blanca Formation, a member of the Ogallala Group. The foci of this study were a micritic ooid layer and a directly overlying stromatolite layer, which crop out in a canyon approximately 10 kilometers west of Channing. Research was conducted primarily using petrographic and scanning electron microscopy.

Significant conclusions include: organic matter was preserved in ooids as filaments and nanoscale spheroids, which served to capture ostracode carapaces within ~10% of micritic cortices; and stromatolites were deposited within an evolving alkaline lacustrine environment producing discernible zones.

Potential significance includes improving the understanding the role of organic matter in calcium carbonate precipitation, which has plausible applications in medical, industrial, and academic realms.

## DEDICATION

This work is dedicated to my immediate family. To my father, Dean, who always brought home cool rocks for us to analyze ever since I can remember. To my mother, Cabrina, who always planned wonderful vacations to locations I would later find in my geology textbooks. And to my younger brothers, Lyle, Lyndon, and Brantley, who always made me play in the dirt.

## ACKNOWLEDGEMENTS

First and foremost, I would like to thank my parents and grandparents for their unconditional support throughout my academic journey. Their love was always felt no matter where my travels led me.

I would like to acknowledge the second family I have acquired over my five years at Mississippi State University. I have created lifelong professional and personal relationships with the faculty and numerous fellow students within the Geology Department.

I would like to thank the staff at the MSU Electron Microscopy Center, specifically Amanda Lawrence, for their instruction and guidance in capturing beautiful images of extremely small objects, and for the endless supply of chocolate and candy.

To Dr. Craig Grimes, for increasing my interest and skill in using the petrographic microscope, as well as broadening my knowledge of petrography. Your friendship was unexpected, yet rejuvenated so many things concerning my outlook on geology, as well as life.

I would like to thank Dr. Douglas Kirkland for the first-person perspective he contributed to this project, his phenomenal ability to edit and re-edit, and friendship. I would also like to thank Dr. Richard Moiola, co-discoverer of the project samples, for his

approval and support of the many abstracts submitted to various organizations. Both Drs. Kirkland and Moiola graciously supplied introductory figures and drafts to this project.

To Dr. Darrel Schmitz, one word comes to mind: opportunity. I have received a continuous flow of opportunities during my time here because of you. I have grown tremendously both professionally and personally, and I thank you for the people I have been able to meet, classes I have been able to teach, and places I have been able to visit.

To Dr. Chris Dewey, I cannot express my gratefulness for your friendship, constant mentorship and motivation, and your capability to challenge me daily to think outside of the box. My awareness of life itself has immeasurably increased over my time here due to your knowledge of the earth and the lives within it.

I am personally indebted to Dr. Brenda Kirkland and Dr. Leo Lynch. It is impossible to fully convey my appreciation for their friendship, persuasion to attend graduate school, abundant babysitting opportunities, and their ability to convince me to love a limestone just as much as I love a granite. I would like to thank them and their children for making me feel a part of their family during the time I have spent away from my own family. Their influences touched every aspect of my life, and I would not be the person I am today without them.



## TABLE OF CONTENTS

	Page
DEDICATION .....	ii
ACKNOWLEDGEMENTS .....	iii
LIST OF TABLES .....	viii
LIST OF FIGURES .....	ix
 CHAPTER	
I. INTRODUCTION AND BACKGROUND .....	1
Study Area .....	3
Sample Acquisition .....	4
Lithology .....	6
Ooid Stratum .....	7
Stromatolite Stratum .....	7
Hypotheses .....	8
Significance of Results .....	8
II. LITERATURE REVIEW .....	10
Prior Research .....	10
Environment of Deposition of Study Area .....	11
Ooids .....	14
Micritic Ooids .....	14
Organic Matter and Formation of Ooids .....	14
Stromatolites .....	15
III. METHODS .....	17
Study Area Measurement .....	17
Sample Collection .....	17
Retrieval and Documentation of Pre-Existing Samples and Thin Sections .....	17
Petrography .....	18
Preparation of New Thin Sections .....	19
Analyses of All Thin Sections .....	20

Scanning Electron Microscopy .....	21
Preparation of Samples .....	21
Stromatolite Preparation .....	22
Ooid Preparation .....	23
Viewing of Samples .....	23
IV. RESULTS .....	25
Ooid Layer .....	25
Hand Sample .....	25
Petrographic Results .....	25
Scanning Electron Microscopy Results .....	28
Nucleus .....	28
Micritic Cortex .....	31
Cement .....	32
Stromatolite Layer .....	34
Hand Sample .....	34
Petrographic Results .....	36
Zone 1 .....	39
Zone 2 .....	42
Zone 3 .....	43
Scanning Electron Microscopy Results .....	44
V. DISCUSSION .....	47
The Role of Organic Matter in the Channing Ooids .....	47
Nucleus .....	47
Micritic Cortex .....	47
Cement .....	48
The Role of Organic Matter in the Channing Stromatolites .....	49
Environment .....	50
Ostracodes .....	50
Stromatolite Zoning .....	51
Abiotic vs. Organic Origins .....	51
VI. CONCLUSIONS .....	53
REFERENCES .....	54
APPENDIX	
A FIGURES AND TABLES CITED .....	57
Figures Cited .....	58
Tables Cited .....	60

B	PERSONAL COMMUNICATIONS.....	61
	Personal Communications .....	62

## LIST OF TABLES

TABLE	Page
1 Point Count Results on Ooid Layer Thin Sections .....	27
2 Point Count Results on Stromatolite Layer Thin Sections .....	40

## LIST OF FIGURES

FIGURE	Page
1 Location of study area.....	2
2 Measured section of Rita Blanca Lake Deposits. Applicable strata denoted. ....	5
3 Ooid layer superimposed by stromatolite layer. Stromatolite indicated by arrow .....	7
4 Cenozoic Stratigraphy of the Southern High Plains (Modified from Frye and Leonard, 1957, and Evans and Meade, 1945).....	13
5 Stromatolite A.....	19
6 Stromatolite B .....	20
7 Field Emission Scanning Electron Microscope at the Electron Microscope Center, Mississippi State University, Mississippi State, MS.....	22
8 Ooid layer hand sample .....	26
9 Digital scan of smooth cut sample from the ooid layer .....	26
10 Ostracode carapace incorporated within micritic coating (PPL) .....	28
11 Nucleus (N), micritic cortex (M), and cement (C) zones within an ooid .....	29
12 Filamentous microbial remnants (F) within the micritic cortex (M) of an ooid sample .....	29
13 Representative ooid nucleus (weathering feldspar) .....	30
14 Boundary between micritic cortex (M) and quartz nucleus (N) .....	31
15 Example of sparry calcite cement in ooid layer.....	32
16 Examples of smooth (S) and irregular (I) crystal faces within a single sparry calcite crystal in ooid cement.....	33

17	High magnification image of bacteria-shaped bodies found on an irregular crystal face of a calcite crystal in ooid cement. ....	33
18	Stromatolite hand sample with three zones indicated.....	34
19	Upper surface of a stromatolite exhibiting a darker surface color compared to others.....	35
20	Sample exhibiting abundant void spaces distributed within the middle section of a cut stromatolite sample .....	36
21	Example of homogenous micrite (PPL).....	37
22	Example of peloidal micrite (PPL) .....	37
23	Example of thrombotic micrite (PPL) .....	38
24	Example of dendritic micrite (PPL).....	38
25	Thin section of a stromatolite depicting the three distinct zones.....	41
26	Geopetal structure within Zone 1 of a stromatolite sample (PPL).....	42
27	A porous Zone 2 within a stromatolite sample .....	43
28	Distinct growth bands (indicated by arrows) within Zone 3 of a stromatolite sample .....	44
29	Globular textures dominate on broken stromatolite surface .....	45
30	Rod-shaped bacteria (indicated by arrows) located on broken stromatolite surface .....	45
31	Fossilized microbial mucilage found in a stromatolite sample.....	46

## CHAPTER I

### INTRODUCTION AND BACKGROUND

The study completed several objectives concerning the Channing Lake Beds: described the internal structure and external morphology of the Channing stromatolites; proposed a role organic matter plays in formation of the micritic ooids; and proposed oolite formation methods and a paleo-environment during oolite and stromatolite deposition.

The Channing lake beds are located in the northwestern part of the Panhandle of Texas, approximately 10 km (6 mi) northwest of Channing, Texas; which is approximately 80 km (50 mi) northwest of Amarillo, Texas. The study area is in Hartley County, Texas, and is located within the geographical province of the High Plains of Texas (Fig. 1). The strata applicable to this study are exposed in tributaries of the Rita Blanca Creek and in road cuts on Texas Farm Road 767.

The lake beds are exposed where streams have eroded the uppermost strata mantling the High Plains. “Caprock”, a widespread layer of caliche (dense calcium carbonate developed by soil-forming processes), is absent in the immediate area of the lake beds (Brown, 1956). During its maximum development, an ancient lake, called Rita Blanca, apparently had an elliptical shape with a north-south length of approximately 10 km (6 mi), and a breadth of roughly 5.5 km (3.5 mi) (Anderson and Kirkland, 1969).

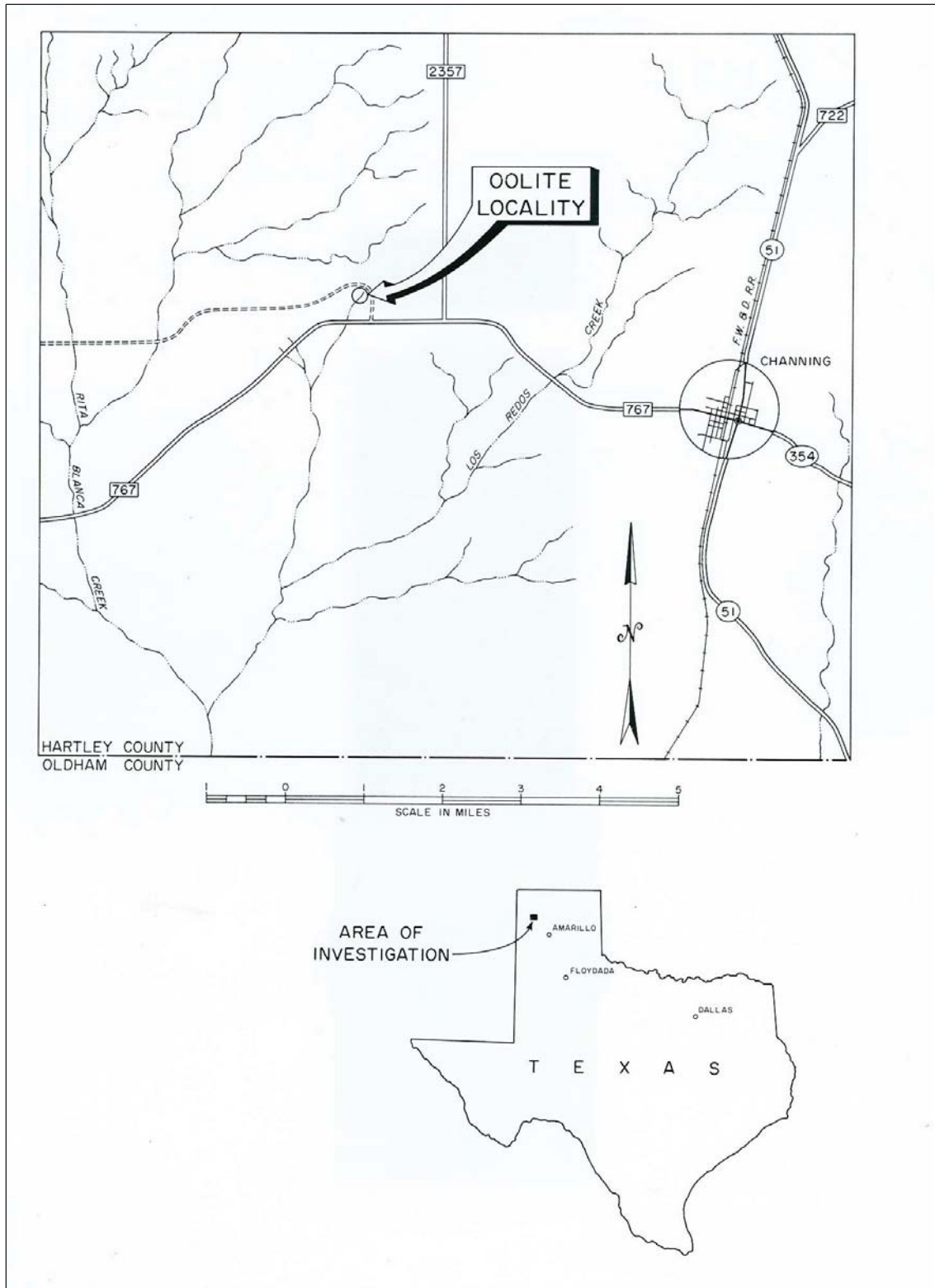


Figure 1 Location of study area



The beds documented in detail herein are the younger portion of the Rita Blanca complex of lake beds described previously (Anderson and Kirkland, 1969). The lake basins may have formed by collapse of sediments of the Pliocene Ogallala Group as Permian halite dissolved in the subsurface. The beds termed “Channing Lake Beds” may be a collection of lake beds of Pliocene and Pleistocene age in a basin that slowly evolved as Permian salt, and to a much lesser extent, Permian anhydrite, dissolved (Dr. Douglas W. Kirkland, personal communication).

As the salt dissolved into water undersaturated with halite (NaCl), the specific gravity of the brine increased and slowly drained into the deeper parts of the Anadarko Basin, an expansive basin partially located within the Texas Panhandle. As the salt dissolved, voids were created and, as collapse occurred, a basin slowly formed at the surface. In pluvial times, water accumulated in these topographic lows forming lakes. As the ground subsided, these lows were filled with lake beds (Dr. Douglas W. Kirkland, personal communication). Today, the Anadarko Basin contains a prolific natural gas reserve and several iodine-rich extraction wells related to the brine. It is the only commercial producer of iodine in the United States (New Mexico and Arizona Land Company, LLC, 2009).

### **Study Area**

The Channing Lake Beds are named after their proximity to the small town of Channing, Texas. Although not particularly pertinent to the geology of the lake beds, its history is interesting. Channing was originally named Rivers, after the railroad paymaster George Channing Rivers. The postal authorities rejected this name in 1888

when it became known that a city of Rivers, Texas already existed. Later that year, the name was subsequently changed to Channing. In 1900, after two separate elections, Channing, instead of Hartley, Texas, was established as the county seat of Hartley County. Development of the city of Channing owes much to the XIT ranch, an expansive property that included parts of ten counties in the Panhandle during the peak of cattle ranching in the area (Channing, Texas: History, 2009). At the last census, the population of Channing stood at 350 residents (United States Census Bureau, 2002).

The Rita Blanca lake beds are also termed the Rita Blanca Formation. The term *Blancan* also refers to a time unit. The Blancan age covers from approximately the mid-Pliocene epoch to the early Pleistocene epoch. The units being investigated probably fall near the top of Blancan time and may conceivably be even younger.

Many sites in the area bear the name of Blanco, such as Mount Blanco and Blanco Canyon. The labeling of sites as “Blanco” has been used since the early 1890s when the Geological Survey of Texas first characterized the formation (Cummins, 1891). In Spanish, *blanco(a)* is translated as “white”. The white lakes are composed of light-gray fine grained mudstone, sandstone, and some conglomerate; hence, *blancan*. The clastic sediments are white because of reduction of ferric oxide by organic matter that is dispersed within the lake beds.

### **Sample Acquisition**

The earliest known geological exploration of the area was by G. L. Evans and G. E. Meade, who provided the first general description of the lake bed deposits. They

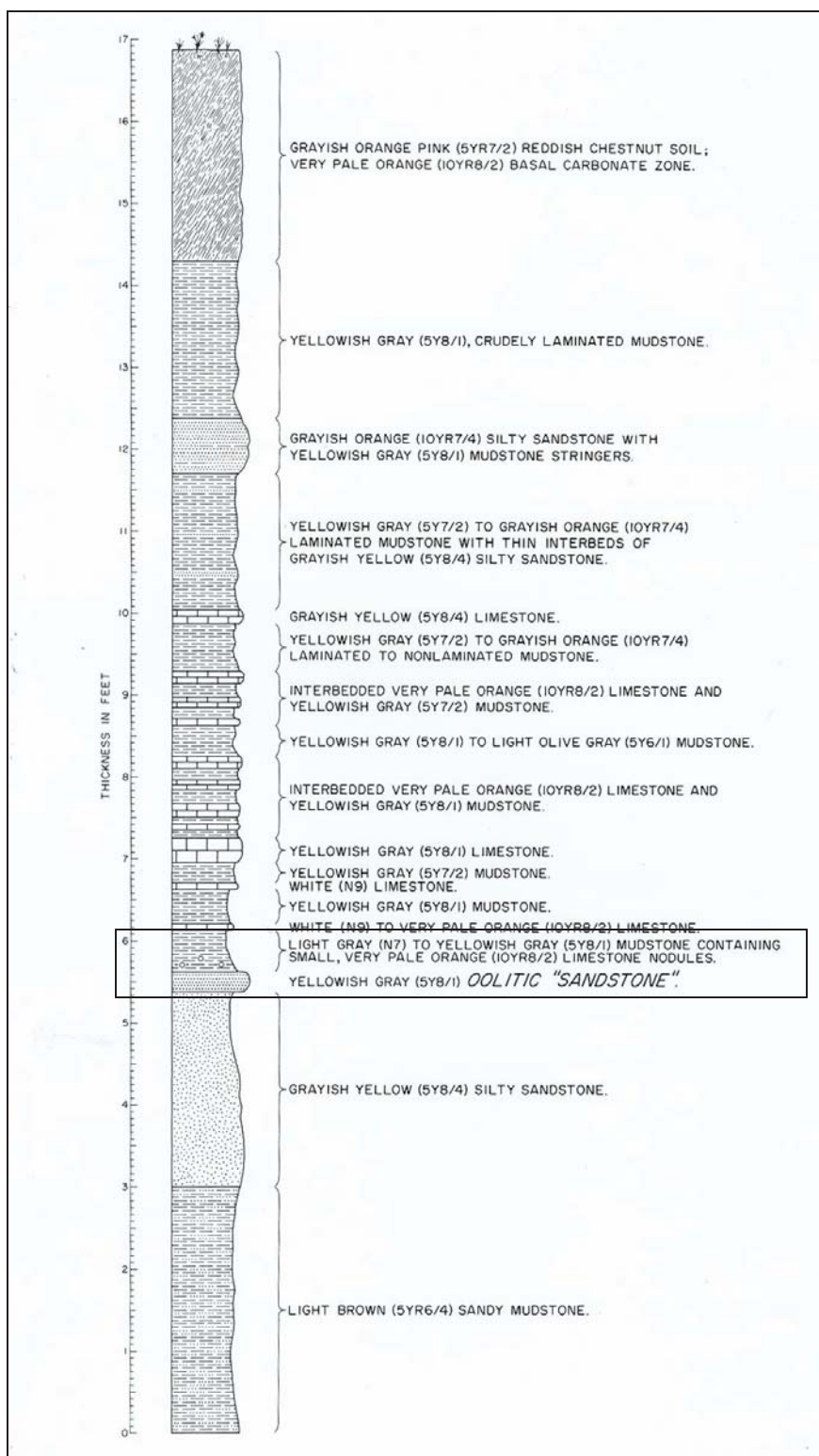


Figure 2 Measured section of Rita Blanca Lake Deposits. Applicable strata denoted.

determined that the Blanco beds of nearby Crosby County, Texas, were laid down in a lake basin (Evans and Meade, 1945). Recognition of a lacustrine origin for these beds led to a search for, and the discovery of, other ancient filled lakes including the Rita Blanca deposits (Anderson and Kirkland, 1969).

Drs. Roger Y. Anderson and Douglas W. Kirkland began their study of a laminated, fossil-rich sequence of the Rita Blanca lake bed deposits in 1960 when they were approached with samples from the area collected by Jerry Harbour of the United States Geological Survey. Harbour had previously extracted pollen from the laminated samples, which was a catalyst for the research later conducted and published by Anderson and Kirkland (1969).

The section applicable to this study was originally measured in 1973 by Drs. Richard J. Moiola and Douglas W. Kirkland (Fig. 2). The samples they collected from this section included an ooid-bearing limestone layer. In 1993, Drs. Brenda L. Kirkland and Douglas W. Kirkland returned to the locality where they discovered stromatolites directly above the ooid-bearing limestone layer. The extensive samples collected during these field trips were the foundation for this study.

### **Lithology**

The column of sediment at the oolite locality is approximately 1.5 m (4.5 ft) and is exposed laterally for roughly 300 m (~300 yds) (Fig. 2). Well below the ooid bed is the thin laminated section of lacustrine clay that is rich in flora and fauna (Anderson and Kirkland, 1969). In this study, I will describe and analyze approximately 23 cm (9 in) of

the 1.5 m column. Within these 23 cm, a distinct stromatolite layer is superimposed on an ooid layer (Fig. 3).



Figure 3 Ooid layer superimposed by stromatolite layer. Stromatolite indicated by arrow.

### **Ooid Stratum**

The ooid layer of the section initially peaked interest with Dr. Douglas W. Kirkland in 1973 when several species of ostracodes were discovered within the cortices of the ooids. One of the ostracode forms can be identified to the generic level in thin section based upon a distinctive undulation of its carapaces (Benson, 1969).

### **Stromatolite Stratum**

The stromatolite stratum was first labeled as a “nodular limestone layer” in both the 1969 publication by Drs. Anderson and Kirkland, as well as the section measured by

Drs. Moiola and Kirkland in 1973. Casual observation of the “nodules” by Dr. Brenda L. Kirkland in 1993 resulted in the recognition of the samples as stromatolites.

### **Hypotheses**

It is proposed that the outer surface of the ooids were coated with organic matter, possibly living algae and/or bacteria and associated mucilage, prior to deposition. The organic matter may have been a living biofilm of algae, and/or bacteria and associated mucilage, and/or archaea. The organic matter coating the ooids probably acted as an adhesive that allowed ostracode carapaces to be integrated into the ooid cortices during agitation of the lake water. It is also proposed that the stromatolites were formed in a stressed environment. The main hypothesis tested by this study states that algae and bacteria were primary agents in the formation of both the ooids and the stromatolites.

### **Significance of Results**

The study has shown the specific role that organic matter played in forming the stromatolites and micritic ooids of the Channing Lake Beds. The significance lies in the possibility of understanding of how the stromatolites and ooids formed in this particular lacustrine environment. It may also reflect on how these features form in other environments. The hypothesis, strictly applied to this particular study, tentatively denotes that organic matter plays a significant role in the precipitation of the ooids. Investigation of the Channing Lake Bed stromatolites may provide a better understanding of the relationship between organic matter and alkalinity of an environment in terms of calcium carbonate precipitation.

Aspects of this study are directly applicable to other areas of geological research, spanning a large temporal and spatial extent, from the search for life on other planets to the most recent petroleum discoveries in South America. The significance of this study may include providing climatological information of the High Plains of Texas during the Pleistocene epoch. The study provides a valuable contribution to the existing understanding of the balance between microbial and chemical environments. The broader impact of this research lies in the possibility of improving the understanding of the role of organic matter in precipitation of calcium carbonate, which has applications in medical, industrial, and other academic realms.

## CHAPTER II

### LITERATURE REVIEW

#### **Prior Research**

In 1969, Drs. Douglas W. Kirkland and Robert Y. Anderson co-authored Paleoecology of an early Pleistocene Lake on the High Plains of Texas. The Geological Society of America Memoir concentrates on the paleoecology, palynology, and paleolimnology of a short section [approximately 1.5 m (4.5 ft)] of laminated Rita Blanca lake deposits. The laminated section formed when the paleoenvironment of the lake greatly differed from the paleoenvironment during oolite deposition. In addition, the fossil-bearing, laminated section is deeper and older than the oolite bed. Unfortunately, the strata separating the two units are unexposed. Both units, however, are clearly part of the spectrum of lake beds that constitute the Rita Blanca lake beds. Interestingly, varve layers contain at least one of the same ostracode genera that occur within the ooid stratum.

The sole publication containing significant information regarding the Channing Lake Bed is that by Anderson and Kirkland (1969). I have had the opportunity to consult with Dr. Douglas W. Kirkland about the nature of the lake beds throughout the course of my research.



### **Environment of Deposition of Study Area**

A complex of fluvial sediment from the Rocky Mountains was deposited on the High Plains during late Miocene? and Pliocene time. These deposits, termed Ogallala Group, generally consist of fine- to medium-grained sand and local gravel deposited on an erosion surface developed on the Mesozoic and Permian rocks (Frye and Leonard, 1957). The sand upon which the Rita Blanca ooids formed was probably derived from the Ogallala sands. In the Panhandle of Texas, the thickness of the Ogallala Group ranges from 15 – 100 m (50 to 350 ft) (Evans and Brand, 1956).

The uppermost unit of the Ogallala Group is a flood-plain channel complex that buried all elements of the former topography. At the top, a caliche soil horizon containing up 60% calcium carbonate is present (Frye and Leonard, 1965). The soil horizon may have been the original source of the calcium that precipitated as calcium carbonate in the lake in which the ooids and stromatolites formed.

Stream deposition in the Panhandle area essentially ended near the end of the mid-Pliocene as a result of an increasingly arid climate and stream piracy (Evans and Brand, 1956). During the upper Pliocene, the “caprock” was developed on a featureless plain (Brown, 1956). During this period of stability, the surface of the High Plains was modified by the formation of deflation basins. These basins were further enlarged by herds of buffalo. In an attempt to get water in an incipient pond, buffalo would trample vegetation at the pond edges. Upon drying, water in the pond receded and would dry the soil. Any surface without a vegetative cover was susceptible to deflation. In this fashion, a wallow would continue to expand until it covered a substantial area (e.g. an acre more or less) (Douglas W. Kirkland, personal communication).

The Rita Blanca Basin is probably too large to have formed exclusively by deflation. It probably originated primarily by dissolution of underlying Permian evaporites, chiefly halite, buried beneath the Ogallala Formation (Douglas W. Kirkland, personal communication). Deflation has been active in the southern High Plains during the Holocene. At irregular intervals, the wind-formed basins become playa lakes, but within a relatively short period of time the water evaporates, leaving mud flats exposed to wind activity (Anderson and Kirkland, 1969).

The dry environment of the late Pliocene was interrupted by what is judged to be sharpest climatic change of the late Cenozoic, the Pliocene-Pleistocene age boundary (Aguirre and Pasini, 1985). The initiation of pluvial conditions marks the break between the Pliocene and the Pleistocene in the southern High Plains. It also indicates the end of a dry climate with deflation basin formation and the beginning of a humid climate with the formation of lakes and lacustrine sediments (Frye and Leonard, 1965).

Continental glaciers moved as far south as northeastern Kansas in the Nebraskan glacial age, while in the southern High Plains small deflation basins became small lakes and some evaporite subsidence areas became large lakes. In a survey of the Nebraskan time stage published by Frye and Leonard (1965), no mention was made of the lake deposits, but on other occasions they suggested that the Rita Blanca deposits are of fluvial origin. A variety of life forms and petrographic analyses indicate a lacustrine origin.

During the Kansas glacial age, the lacustrine Tule Formation was deposited in deflation basins in the Panhandle area (Evans and Brand, 1956). In Hartley County, beds age equivalent to the Tule Formation overlie the Rita Blanca deposits. The Pearlette

volcanic ash fell during the lake Kansas glacial or earliest Yarmouthian interglacial and was deposited on the Ogallala Group or on the Tule Formation and its equivalents in the southern High Plains (Frye and Leonard, 1957). The Tahoka Clay, a lake deposit from the Wisconsin glacial age, consists of calcareous, bentonitic clay and sand, and was deposited in all of the large basins and in many of the shallow playas existing on the present High Plains surface (Anderson and Kirkland, 1969) (Fig. 4).

Series	Pleistocene ages	North American ages	Rock unit	Sedimentary environment
Pleistocene	Recent interglacial	Rancholabrean	Dune sand	Aeolian
	Wisconsin glacial		Tahoka Clay	Lacustrine
	Sangamon interglacial			
	Illinoian glacial			
	Yarmouth interglacial	Irvingtonian		
	Kansan glacial		Pearlette volcanic ash Tule Formation	Lacustrine
	Aftonian interglacial			
	Nebraskan glacial	Blancan	Rita Blanca deposit Blanco Formation	Lacustrine
Pliocene	Upper			
	Middle	Hemphillian	Ogallala Group	Fluvial
	Lower			

Figure 4 Cenozoic Stratigraphy of the Southern High Plains (Modified from Frye and Leonard, 1957, and Evans and Meade, 1945)

## Ooids

### Micritic Ooids

According to the Encyclopedia of Sediments and Sedimentary Rocks, ooids lacking an orderly tangential or radial microfabric are described as having a *random microfabric* (Middleton, et. al., 2003). Such ooids are commonly referred to as micritic ooids. Modern ooids generally exhibit a random arrangement of aragonite rods or crystals. A random microfabric is more often a product of micritization, rather than being an original depositional fabric. Micritic ooids have been described from a variety of low and high-energy settings.

### Organic Matter and Formation of Ooids

For over a century, geologists have realized that organic processes, products, and organisms themselves have played a very important role in ooid formation. Processes can range from actual algae and bacteria living within the ooid to borings and mucus layers on and within the ooid down to details of close molecular-level relationship between various organic chemicals and their role in templating the precipitation of calcium carbonate (Folk and Lynch, 1997).

Cyclicity of environments could be determined in the Channing Lake Bed ooids if an ooid exhibiting a low degree of micritization is discovered in thin section. Ooids that distinctly display cyclicity, such as the Bahamian Joulter's Cay ooids, will possess a repetitive pattern in thin section: a crystalline birefringent (aragonite) ring, alternating with an isotropic gap. The gap in most ooids is empty space that was once filled by

concentric layers of organic matter (Folk and Lynch, 2001). Finding such an example would be advantageous in determining the role of organic matter in the formation of the Channing Lake Bed ooids.

### **Stromatolites**

The Channing Lake Bed stromatolites are proposed to have precipitated under lacustrine alkaline conditions ( $\text{pH} > 9$ ) based on a variety of evidence from ostracode, fish, insect fauna, and fossil flora analysis (Anderson and Kirkland, 1969). The literature review of stromatolites has been initially approached from a lacustrine alkaline basis.

The formation of stromatolites includes blue-green algae, also known as cyanobacteria or cyanophytes, trapping and binding sediment it comes in contact with due to wave action, wind action, and other agitation. Stromatolites typically have distinct internal layering because stromatolites grow towards the sunlight. Cyanophytes cannot be exposed for long periods of time and survive; therefore an environment that allows the stromatolite head to be submerged in clear, shallow waters is essential in its formation.

The first stromatolites to be correctly identified as containing and requiring bacteria for their precipitation were entirely marine. Freshwater stromatolites are less abundant than their marine counterparts, and therefore less studied. A comparison may be made between modern microbial mats and stromatolites that inhabit hypersaline and otherwise extreme environments and lacustrine stromatolites that arise during extreme climatic shifts over geologic time (Whiteside, 2004).

The term “lacustrine” implies a lake environment. To be labeled as a lacustrine environment, the involved water is not required to be either fresh, brackish, or saline.

The only requirement is to be associated with a lake, generally a restricted body of water, as opposed to being associated with fluvial, deltaic, or marine processes.

The mineralogy of most modern lacustrine stromatolites is dependent on the precipitating carbonate phase within the ambient lake water. This is true even when biotal metabolism plays a significant role in controlling rates of carbonate precipitation. Stromatolites and microbial bioherms are aragonitic in many modern saline lakes, and the precipitation process is often facilitated by the metabolic activities of bacteria (Warren, 2006).

Certain textures exhibited by minerals precipitating in alkaline lacustrine environments can be applied to stromatolites forming under the same conditions. When a mineral is precipitated under alkaline lacustrine conditions and is subsequently dehydrated due to evaporation, it alters from generally soft, plastic white paste to “crocodile-skin” or a cracked appearance. This texture is used to support an alkaline lacustrine interpretation in ancient rocks (Warren, 2006).

## CHAPTER III

### METHODS

#### **Study Area Measurement**

The oolite study area was measured by Drs. Richard J. Moiola and Douglas W. Kirkland in the latter half of 1973. The section is contained within the oolite locality (Fig. 1), and extends laterally roughly 270 meters (~300 yds) and vertically one and 1.5 m (~4.5 ft).

#### **Sample Collection**

Hand samples were collected from the oolite locality in 1993 and 1994 by Drs. Douglas W. Kirkland and Brenda L. Kirkland. The samples were sourced from the ooid layer and the superimposing stromatolite layer. Float pieces as well as soil samples were also collected at different locations around the study area. The stromatolites are located south of the oolite bed exposure in road cuts along Texas Farm Road 767.

#### **Retrieval and Documentation of Pre-Existing Samples and Thin Sections**

All hand samples and soil samples from the 1993 and 1994 field trips were obtained from Storage Building A on Buckner Lane, Mississippi State, Mississippi, at the

end of summer 2008. Pre-existing thin sections from these samples were obtained from Dr. Brenda L. Kirkland at approximately the same time.

Each hand sample was appropriately labeled and categorized dependent on its location in the measured section. Most hand and soil samples were given a unique number based on day, month, year, and time collected. The number allowed for the samples to be assigned a specific number which cannot be duplicated. The day, month, and year without hyphens or slashes is followed by the time using the 24-hour designation. Thus, a sample labeled as 627931323 was collected on June 27, 1993, at 1:23pm. This system of numbering is extremely effective and yields a unique number for each sample (Brenda L. Kirkland, personal communication).

Three stromatolites samples were labeled as A, B, and C. Stromatolite C had pre-existing thin sections from 1994. Five thin sections from different layers of stromatolite C were digitally scanned at high resolutions for more precise observations, as well for “mapping” the internal structure of the stromatolite.

### **Petrography**

Petrographic analysis of the samples from the Channing Lake Bed provided a significant portion of the information obtained for this study. Information obtained from petrographic analysis cannot be derived from other methods. Petrography allowed reconstruction of stromatolitic structures and the positive recognition of ostracodes in the cortices of the micritic ooids.



### Preparation of New Thin Sections

Stromatolites A and B were selected for preparation of new thin sections. Selection was based upon their stable and rigid appearance, and hence, the assumption they would stay intact throughout the sawing process. An MK212 Wet-Cutting Table/Stone Saw was used to cut the samples. Stromatolite A was sliced into four pieces (Fig. 5). Stromatolite B was also sliced into four pieces. During the cutting process, Stromatolite B fractured perpendicular to the cutting direction, resulting in a total of five pieces (Fig. 6).

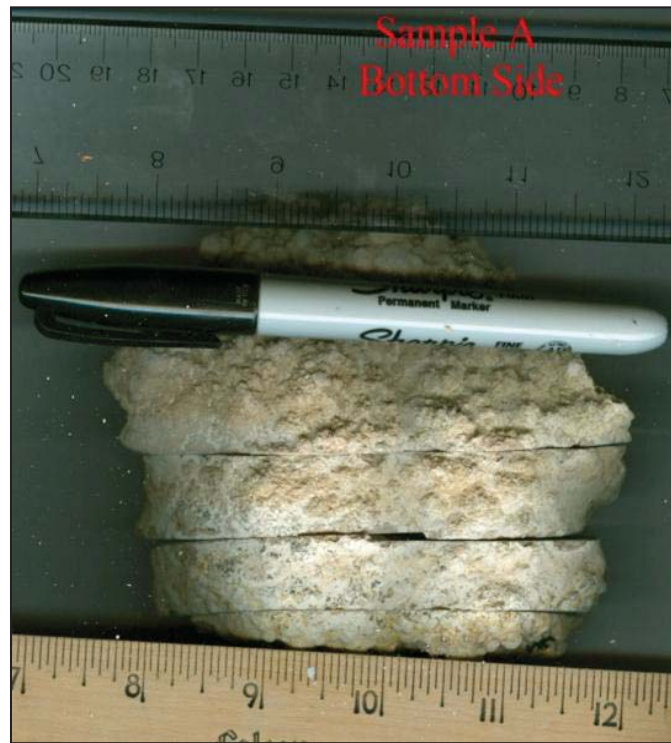


Figure 5 Stromatolite A



Figure 6. Stromatolite B

### **Analyses of All Thin Sections**

Thin sections from stromatolites A, B, and C were “mapped” in an effort to determine layering patterns and location of ostracode carapaces. In addition, thin sections from the oolite layer were analyzed for occurrences and locations of ostracode carapaces within ooid cortices. Point counts were completed on both the stromatolite thin sections as well as the oolite thin sections to determine any patterns or associations.

R. L. Folk’s “white-card technique” is a method in which organic matter can be easily detected in thin section. A white piece of paper is placed underneath a thin section and an external light source is directed onto the thin section. The external light from above and white paper underneath allows organic matter to appear highly reflective in the microscope (Folk, 1987). A modified version of Folk’s “white-card technique” was

applied to the Channing stromatolite thin sections. The modified version, known as the “blue-card technique”, uses a blue-colored card (Milliken, 2005). The blue color enhances the reflectivity of the organic matter allowing it to be more easily recognized.

The ostracodes, including the genus *Limnocythere*, provided an important portion of paleoenvironment information. This aspect of the study was casually pursued, as most analysis of the ostracodes has already been completed for Drs. Anderson and Kirkland by Dr. Richard Benson (Benson, 1969). The analysis was used as additional evidence to confirm environmental conditions of the stromatolites and ooids.

### **Scanning Electron Microscopy**

The scanning electron microscope used for this study is a Field Emission Scanning Electron Microscope located at the Electron Microscope Center (EM Center) on the campus of Mississippi State University in Mississippi State, Mississippi (Fig. 5). The field emission scanning electron microscope (FESEM) has a magnification range of 10X to 500,000X. The resolution varies dependent upon the selected accelerating voltage, which can range from 1 kV to 20 kV. At an accelerating voltage of 15kV, the resolution of the secondary electron image is 1.5 nanometers. At an accelerating voltage of 1 kV, the resolution of the secondary electron image is 5.0 nanometers (Field Emission Scanning Electron Microscope Specifications, 2009).

### **Preparation of Samples**

Scanning electron microscopy is conducted in a vacuum; otherwise gas molecules would interfere with the electron beam of the microscope and disturb the backscattered

electrons used for imaging. To further reduce interference with the electron beam, samples are typically coated with a thin layer of alloy to reduce the electron absorption capability of the sample. Electron absorption within a sample results in an imaging hindrance known as “charging”. The coating of the samples allows the electrons to reflect back to the microscope producing an image of the sample surface.



Figure 7 Field Emission Scanning Electron Microscope at the Electron Microscope Center, Mississippi State University, Mississippi State, MS

### *Stromatolite Preparation*

Remaining saw cuttings of Stromatolites A and B were the first samples to be chosen for viewing with the FESEM due to their size and abundant broken surfaces, ideal for obtaining genuine data. Five pieces were attached to stubs using a silver paste. After the silver paste dried, a gold coating was applied to the samples by a palladium/gold sputter coater. The ratio of gold to palladium is 60:40. The layer is generally 10 - 20 nm

in thickness and applied evenly allowing for a true image of the sample surface. Coating lasted thirty seconds for the stromatolite samples. It should be noted that gold coating in excess of one minute can result in false textures on the sample surfaces resembling bacterial origins and/or bodies. In this organics-focused study, these “Au-artifacts” would void any data acquired through viewing any excessively coated samples (Folk and Lynch, 1997). Therefore, the minimum coating was chosen even though charging was sometimes problematic.

### *Ooid Preparation*

Samples from the oolite layer were selected based on projected stability during the sawing process. Using the same table saw which cut the stromatolites, three 1 in (2.5 cm) blocks were produced for SEM viewing. Each of the three blocks were uniquely prepared to produce three different viewing surfaces. These preparations included a broken surface, an etched surface created by a 10 second exposure to hydrochloric acid, and a smooth surface produced by the table saw. After mounting with hot glue, the samples were coated with gold/palladium for 30 seconds to inhibit any artifact production (Folk and Lynch, 1997).

### **Viewing of Samples**

The ooid and stromatolite samples were viewed under an average magnification of approximately 16,000X. The viewing magnification ranged from 50X to 130,000X. The customary accelerating voltage is 5kV. Only during instances of excessive charging was the accelerating voltage decreased. The working distance varied from 15 mm –

40mm depending upon magnification and resolution desired. Valuable images were saved to the desktop hard drive and later transferred to a compact disc or digital flash drive for archiving.

## CHAPTER IV

### RESULTS

#### **Ooid Layer**

The ooid layer *in situ* crops out approximately three-quarters above a ravine bottom revealing an approximately 10 cm (4 in) thick bed. The ooid layer is well-cemented and stands in relief creating a ledge. The exposure of the layer continues approximately 300 m (~300 yds). It is overlain by the stromatolite layer (Fig. 2, Fig. 3).

#### **Hand Sample**

In hand sample, the texture and appearance of the ooid layer is very similar to a quartz sandstone due to the small size of the ooids (Fig. 8). The layer is moderately to well-cemented and varies in color from white to pale pink, gray, and, in some examples, yellow. When cut by a table saw for further examination and sample preparation, the resulting smooth surface distinctly exhibited a well-sorted, well-cemented ooid layer (Fig. 9).

#### **Petrographic Results**

A petrographic microscope revealed that the ooid layer is composed of micritic ooids, approximately 0.17 – 0.30 mm in diameter, held together by sparry calcite cement.





Figure 8 Ooid layer hand sample



Figure 9 Digital scan of smooth cut sample from the ooid layer

A petrographic point count of five random thin sections from the ooid layer was infrequently detrital zircons and volcanic rock fragments (1%). The siliciclastic nuclei were predominantly sub-angular to sub-rounded grains ranging from 0.001 – 0.62 mm in diameter. The ooid cortices consist of layers of micrite ranging from 0.005 – 0.20 mm in thickness.



In approximately 10% of the ooids, at least one ostracode carapace was incorporated into the micritic coating (Fig. 10). Ostracodes were positively identified by shape and/or by recognizing the undulation of the microstructure within the carapace during stage rotation. From previous studies of these thin sections, the ostracodes were classified as *Limnocythere* sp. (Benson, 1969).

Table 1 Point Count Results on Ooid Layer Thin Sections

Thin Section #	Nuclei Composition	Average Diameter	Angularity	Micrite Thickness	Ostracode w/in Cortex?
136-B	Quartz – 90% Feldspar – 10%	0.302 mm	Angular – 20% Subrounded – 48% Rounded – 42%	0.043 mm	Yes – 14% No – 86%
T-5-S-E	Quartz – 85% Feldspar – 15%	0.225 mm	Angular – 31% Subrounded – 58% Rounded – 31%	0.0792 mm	Yes – 13% No – 87%
T-4	Quartz – 89% Feldspar – 11%	0.257 mm	Angular – 7% Subrounded – 72% Rounded – 21%	0.052 mm	Yes – 9% No – 91%
41892-317	Quartz – 91% Feldspar – 9%	0.262 mm	Angular – 6% Subrounded – 79% Rounded – 15%	0.0614 mm	Yes – 7% No – 93%
41892-517	Quartz – 89% Feldspar – 11%	0.178 mm	Angular – 9% Subrounded – 77% Rounded – 14%	0.0811 mm	Yes – 5% No – 95%

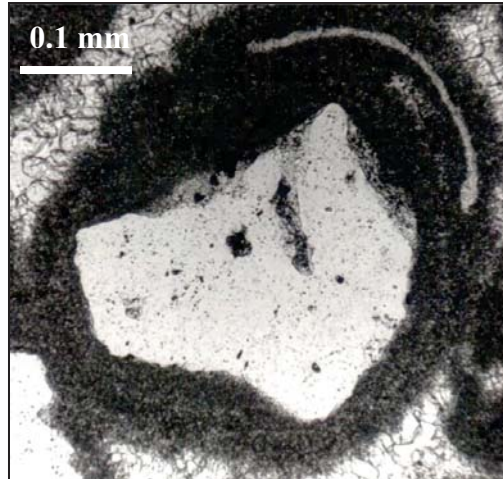


Figure 10 Ostracode carapace incorporated within micritic coating (PPL)

### Scanning Electron Microscopy Results

Scanning electron microscopy was used to image three differently prepared samples: a broken surface, a smoothly cut surface, and an etched surface. The broken surface sample contributed the most information as well as the best images. When viewing ooid samples with a Field Emission Scanning Electron Microscope (FESEM), three zones were apparent within each ooid: nucleus, micritic cortex, and cement (Fig. 11). In some samples, filamentous and fossilized microbial remnants were also visible (Fig. 12).

#### *Nucleus*

The compositions of quartz and feldspar nuclei were re-confirmed by FESEM. Quartz nuclei were relatively smooth in texture and, in some examples, exhibited conchoidal fracture. Most feldspar nuclei exhibited cleavage planes and various degrees of weathering accompanied by remnant microbial filaments. (Fig. 13). Other than

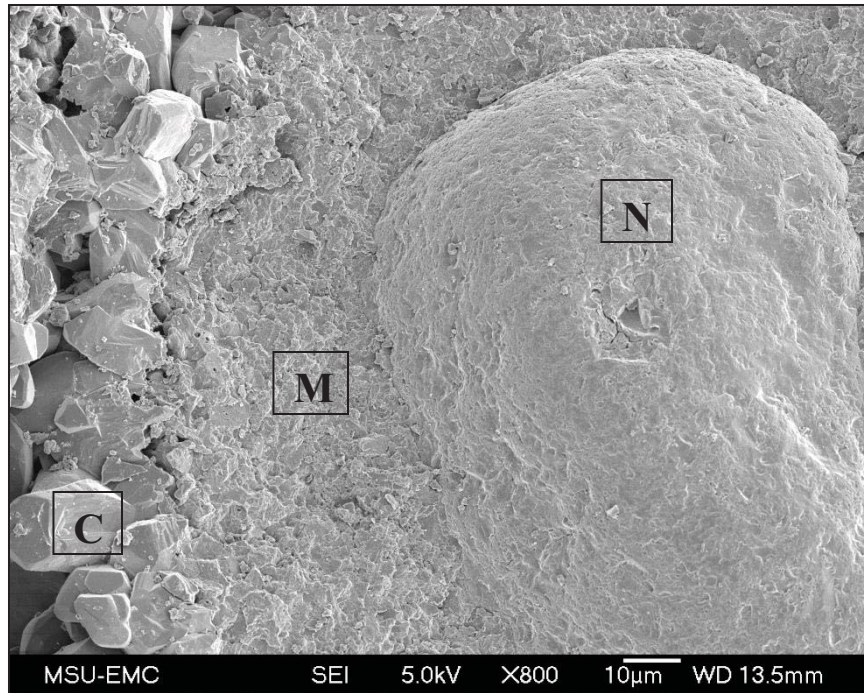


Figure 11 Nucleus (N), micritic cortex (M), and cement (C) zones within an ooid

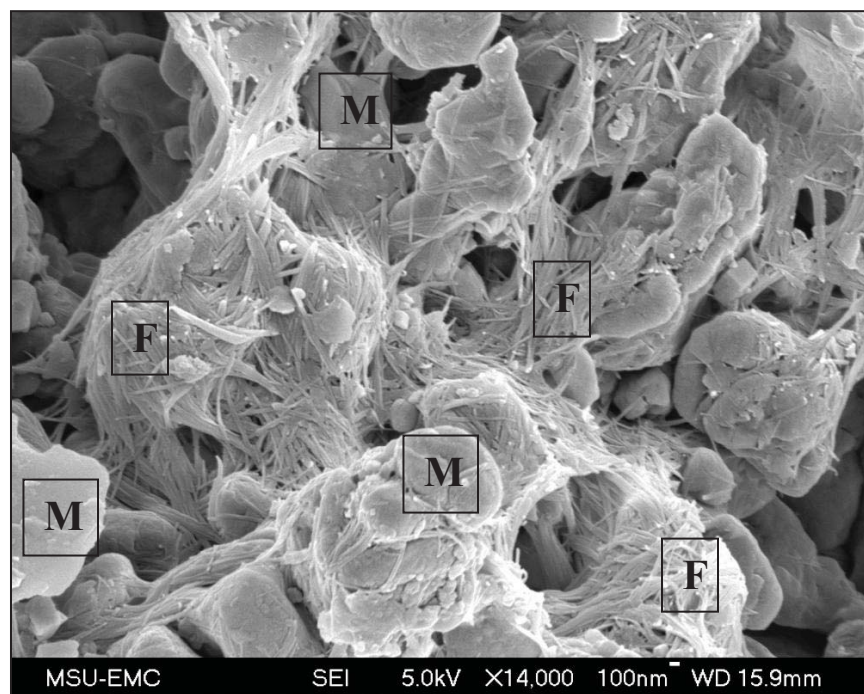


Figure 12 Filamentous microbial remnants (F) within the micritic cortex (M) of an ooid sample

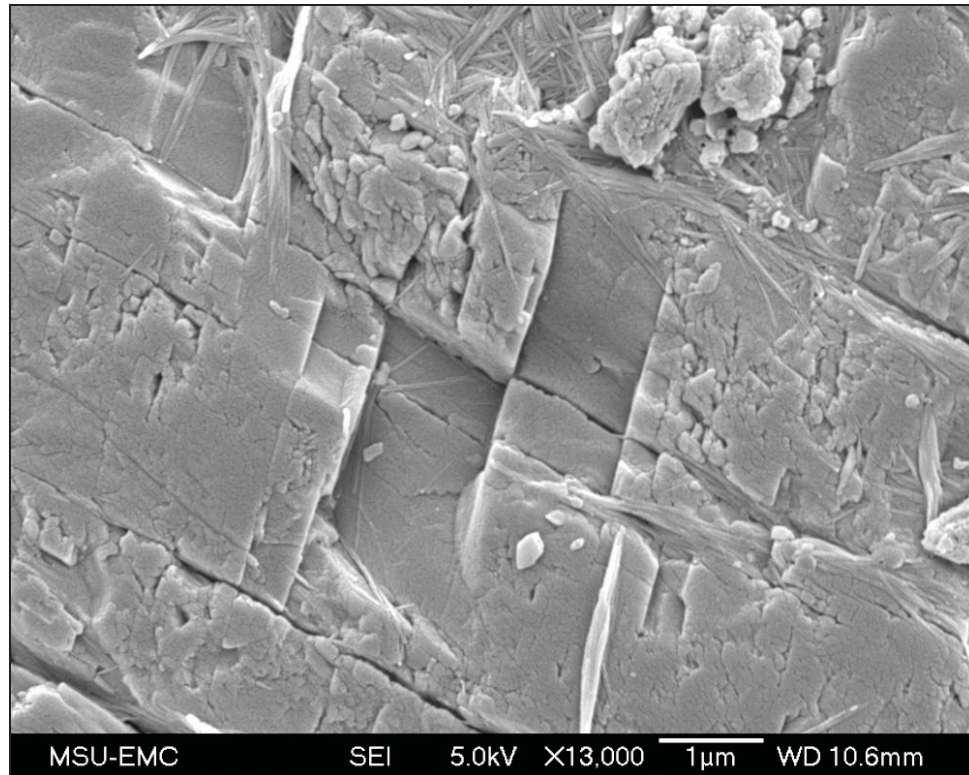


Figure 13 Representative ooid nucleus (weathering feldspar)

weathering features, no organic remnants or filaments were evident within any nuclei examined.

The boundary between a nucleus and the micritic cortex is distinguished by textural and image contrast differences. A quartz nucleus exhibits a smooth weathered surface without cleavage planes, whereas the micritic cortex appears globular and conforms to the borders of the nucleus (Fig. 14).



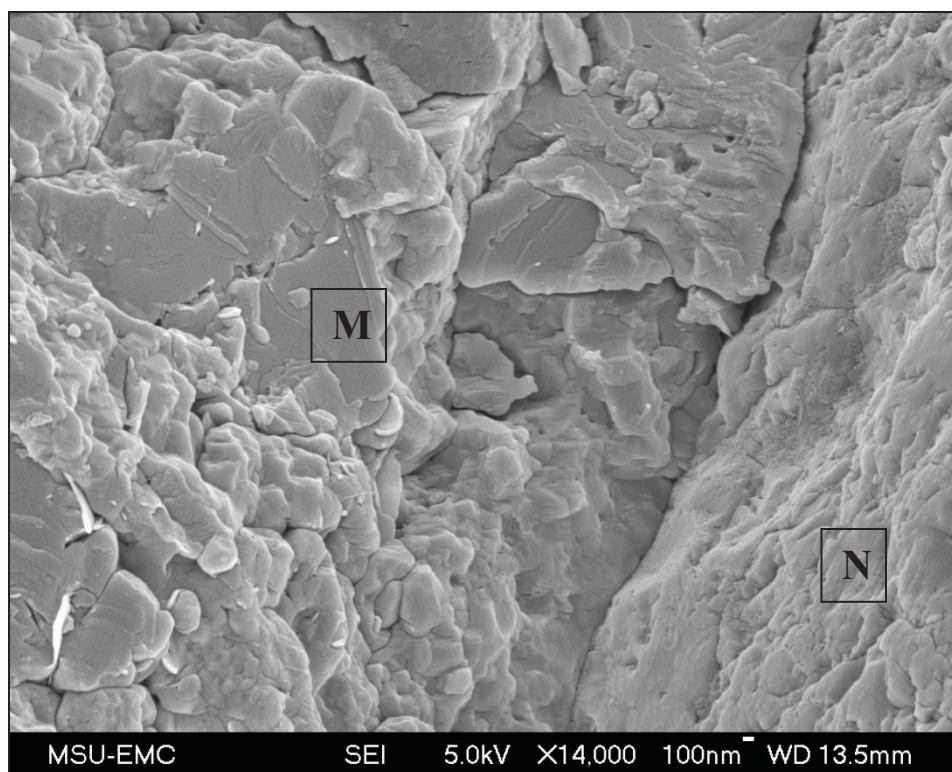


Figure 14 Boundary between micritic cortex (M) and quartz nucleus (N)

### *Micritic Cortex*

The micritic cortex provided the most interesting and plausible data of the three ooid zones. Scanning electron microscopy revealed the cortex was composed dominantly of 200 nm – 2  $\mu$ m diameter spheroids, 300 nm – 2  $\mu$ m long thin filaments, and ~0.1 mm long well-developed microbial mucilage filaments. The cortex material is noticeably different than its neighboring zones based on spheroidal texture and evidence of microbial presence. The micritic cortex is the only zone to possess an abundance of filamentous and/or fossilized microbial remnants (Fig. 12).

## *Cement*

Under a scanning electron microscope at a low magnification, the ooid cement appears to be a typical equant sparry calcite cement with crystals ranging from 10  $\mu\text{m}$  – 100  $\mu\text{m}$  in length (Fig. 15); however, when viewed at  $>10,000\times$  magnification, evidence of some sort of microbial presence was observed. Uneven, irregular crystal face textures were exhibited on some calcite crystals. For example, within a single crystal, certain faces may exhibit a smooth surface, whereas adjacent faces may be uneven and irregular (Fig. 16). In a few instances when viewing at  $>60,000\times$ , elongated bacteria-shaped, rod-like filaments were discovered on the surfaces of calcite cement crystals (Fig. 17).

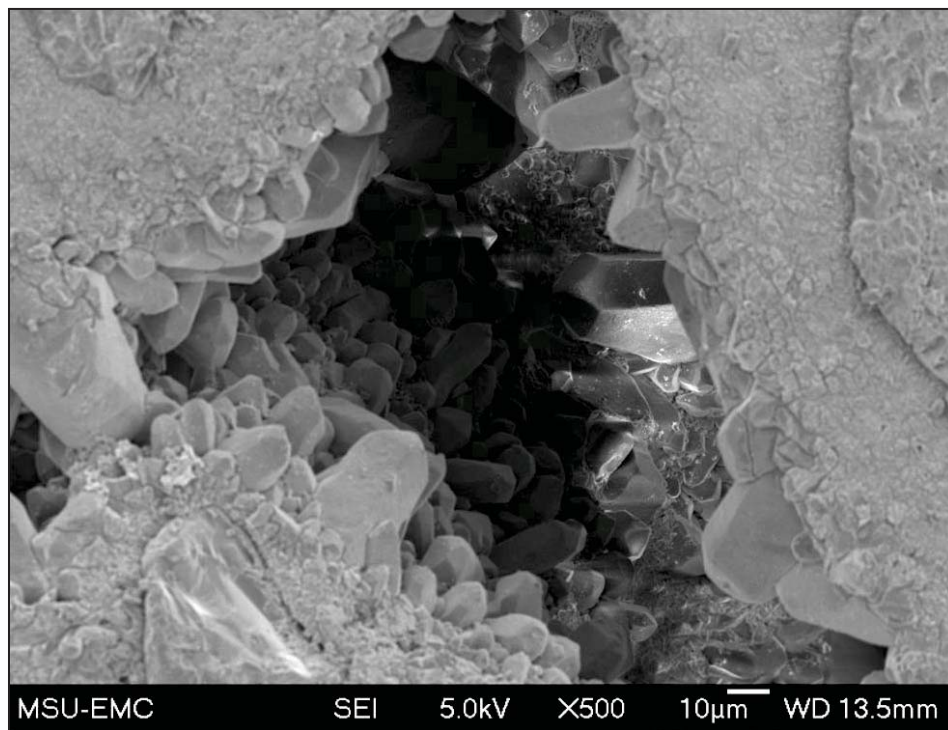


Figure 15 Example of sparry calcite cement in ooid layer

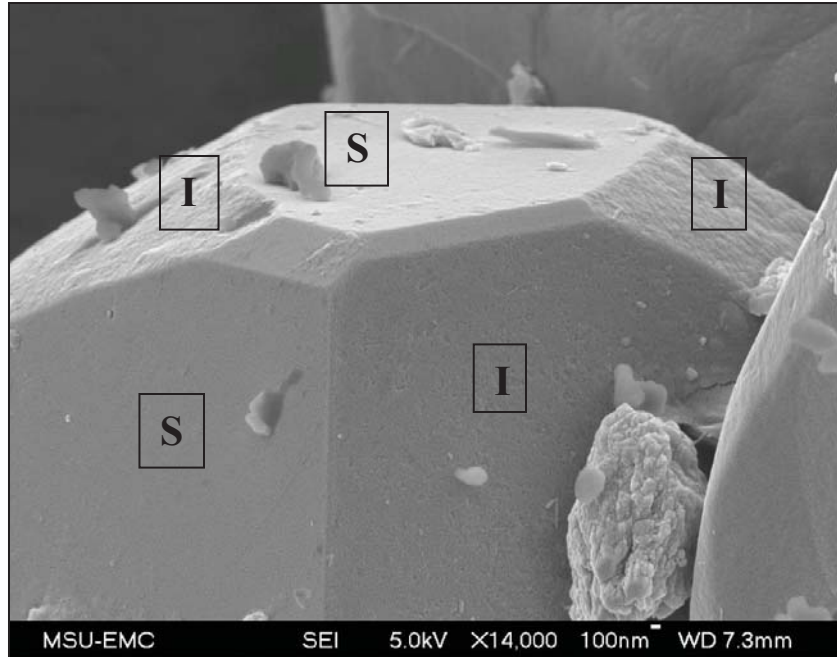


Figure 16 Examples of smooth (S) and irregular (I) crystal faces within a single sparry calcite crystal in ooid cement

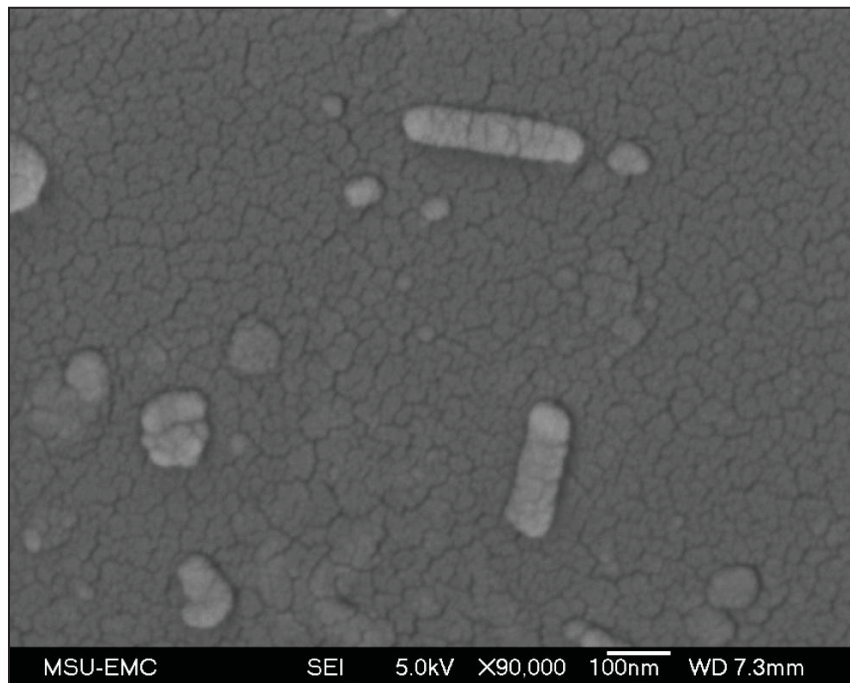


Figure 17 High magnification image of bacteria-shaped bodies found on an irregular crystal face of a calcite crystal in ooid cement

### Stromatolite Layer

The stromatolite layer *in situ* is approximately 12 cm (5 in) and superimposes the oolite layer (Fig. 2). The stromatolite heads range from 6 – 10 cm (2.5 – 4 in) in diameter and stand 2.5 – 5 cm (1 – 2 in) high.

### Hand Sample

In hand sample, the outer surfaces of the stromatolites vary from relatively smooth to knobby and nodular. The stromatolites are visibly more fragile in comparison to the ooid layer. Thickness and length of each sample are proportional and increase or decrease with overall size. When cut length-wise, three distinct zones were evident within the stromatolites due to coloration, texture variations, and distribution of spherical to sub-spherical void spaces (Fig. 18).

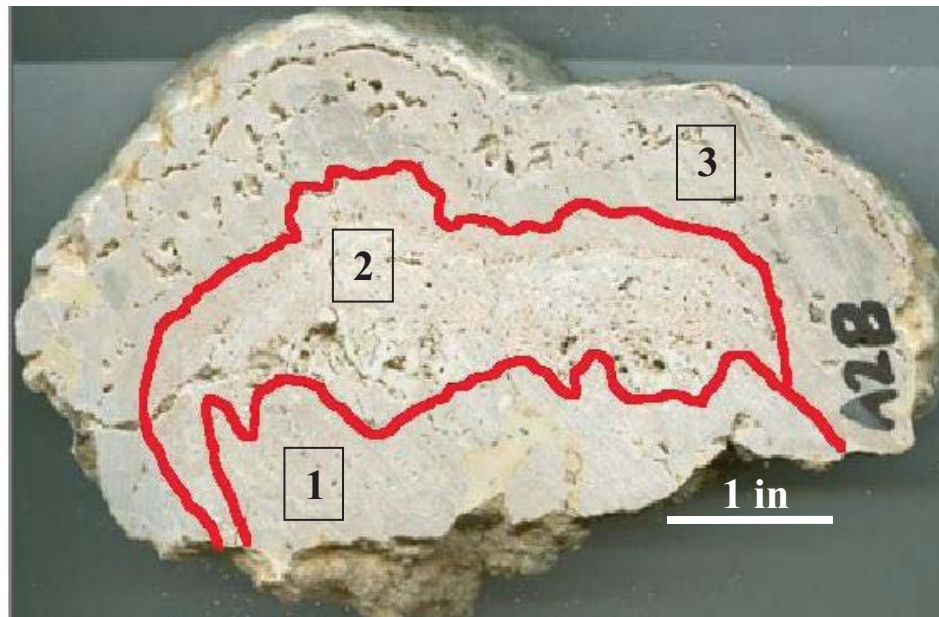


Figure 18 Stromatolite hand sample with three zones indicated



Coloration of the outside surface of the stromatolite heads ranged from chalky white to light and dark tan, with some samples reaching a rusty red hue. A few samples were sporadically covered by a dark brown to black coating (Fig. 19).



Figure 19 Upper surface of a stromatolite exhibiting a darker surface color compared to others

The outer layer of the stromatolites consists of randomly distributed, spherical to sub-spherical nodules which decrease in size as their height increases. Relief exhibited by the small nodules ranges from ~1 – 13 mm (0.05 – 0.5 in) from the surface of the stromatolite. Diameters of the small nodules range from 4 mm – 4 cm (0.15 – 1.5 in).

Void spaces within a cut stromatolite sample display no particular pattern in size, shape, or volume. Areas of abundant void spaces were concentrated within the middle section of each stromatolite (Fig. 20).



Figure 20 Sample exhibiting abundant void spaces distributed within the middle section of a cut stromatolite sample

### **Petrographic Results**

Several types of submicroscopic micrite were recognized within the Channing stromatolite thin sections: homogenous/smooth micrite (Fig. 21), peloidal micrite (Fig. 22), thrombotic/clotty micrite (Fig. 23), and dendritic micrite (Fig. 24) (Riding, 1991). The micrite types varied between zones. Homogenous/smooth submicroscopic micrite was prevalent in Zones 1 and 3, whereas peloidal cement (50 – 250  $\mu\text{m}$  clumps) and thrombotic/clotty micrite (0.1 – 0.5 mm clumps) were more common in Zone 2. Dendritic fabrics were rare, but substantial enough to be noted, specifically in Zone 2.

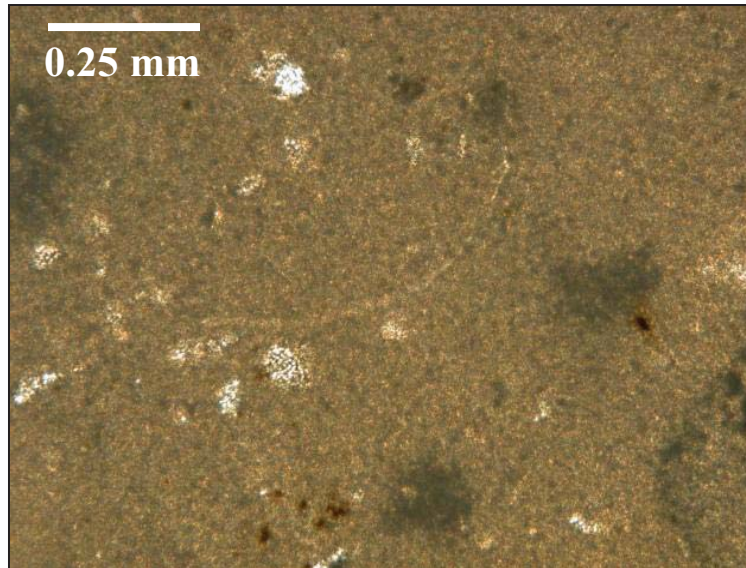


Figure 21 Example of homogenous micrite (PPL)

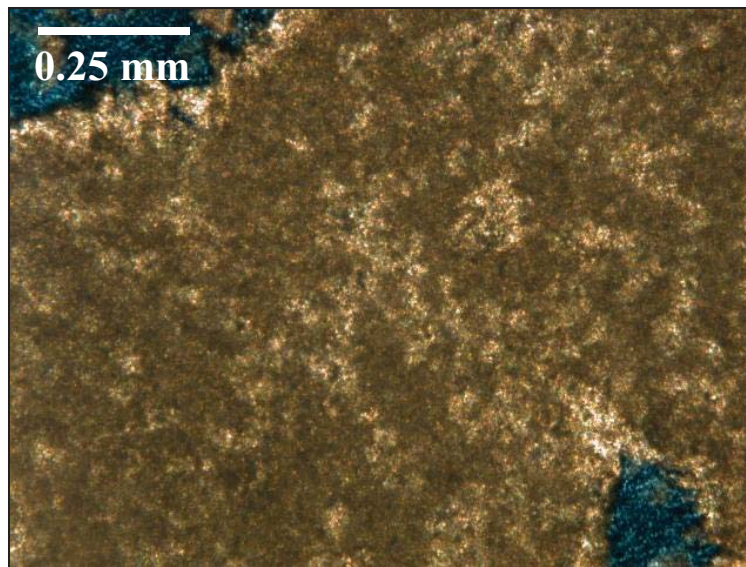


Figure 22 Example of peloidal micrite (PPL)



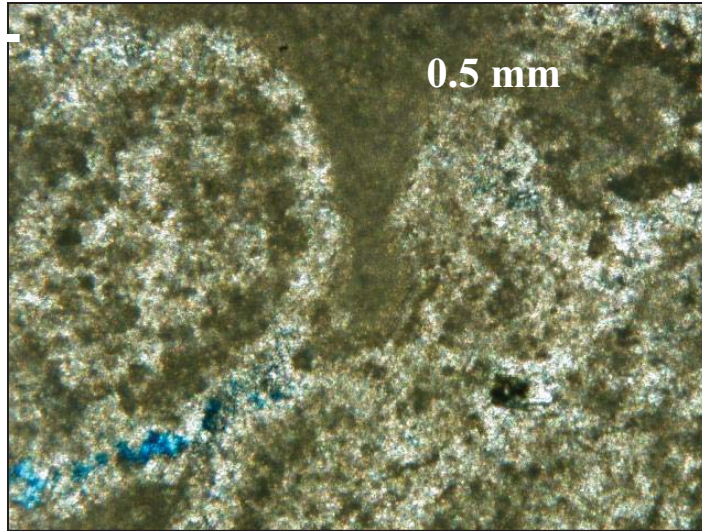


Figure 23 Example of thrombolitic micrite (PPL)

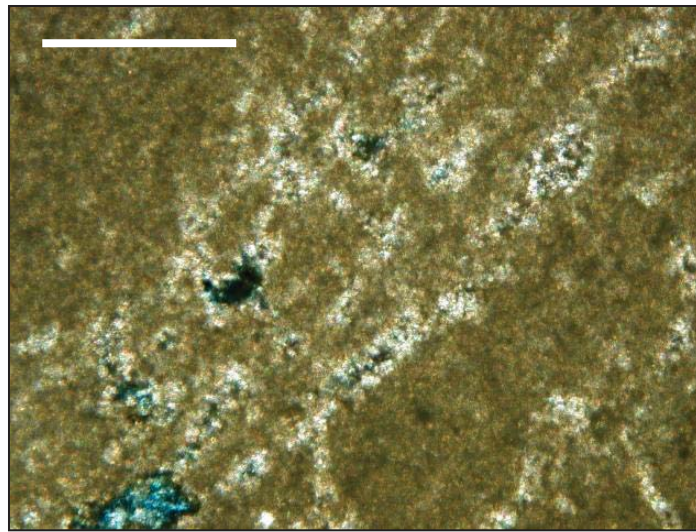


Figure 24 Example of dendritic micrite (PPL)

A petrographic point count of the stromatolite samples was completed in an effort to describe the average composition, dominant micrite type, and numerically compare ostracode-bearing samples to samples in which ostracodes were absent. The point count used two thin sections from Stromatolite A, two thin sections from Stromatolite B, and

one thin section from Stromatolite C. Thin sections were chosen at random and viewed at a magnification of 20X. Thin sections for Stromatolite A and Stromatolite B were each counted 100 points for a total of 400 points. Stromatolite C thin section was counted 200 points. A total of 600 points were counted out of the five thin sections.

The point count resulted in an average composition of 7.5% quartz, 10.3% calcite, and 82.2% micrite. The dominant type of micrite was homogenous (48.7%), followed by peloidal (33.2 %), thrombotic clots (17.9%), and dendritic fabrics (0.2%). Ostracode carapaces were found in 16.8% of the 600 points (Table 2).

Petrographic analysis of the stromatolites also resulted in the confirmation of three separate zones observed in hand sample (Fig. 25). Zone 1 will refer to the original base the stromatolite began to grow upon. Zone 2 will refer to a mid-zone of growth, and Zone 3 will refer to the final, outer growth zones.

### *Zone 1*

Zone 1 possesses abundant ostracode carapaces within the small void spaces. Accumulations of the carapaces and/or micrite within the fabric confirm the direction of stromatolite growth because of a geopetal distribution (Fig. 26). In some areas of Zone 1, the ostracodes have completely infilled void spaces; however, other sections taken from different hand samples do not contain ostracode carapaces at all.

Micrite types for Zone 1 were predominately homogenous/smooth micrite and peloidal micrite. The homogenous micrite areas contained the least amount of color and texture variations. Homogenous micrite areas were smooth, matte brown in color. Areas containing peloidal micrite appeared clumpy. Colors ranged from dark browns to very

light browns. In several areas within Zone 1, alternating zones of peloidal micrite and homogenous micrite were common.

Table 2 Point Count Results on Stromatolite Layer Thin Sections

	Thin Section #	Composition	Micrite Type	Ostracode Present?
<b>Stromatolite A</b>	A3A-2	Quartz – 4% Calcite – 11% Micrite – 85%	Homogenous – 54.1% Peloidal – 35.3% Thrombolitic – 9.4% Dendritic – 1.2%	Yes – 3% No – 97%
	A3A -3	Quartz – 6% Calcite – 8% Micrite – 86%	Homogenous – 69.8% Peloidal – 26.7% Thrombolitic – 3.5% Dendritic – 0%	Yes – 15% No – 85%
	<b>Average (A)</b>	<b>Quartz – 5% Calcite – 9.5% Micrite – 85.5%</b>	<b>Homogenous – 61.95% Peloidal – 31% Thrombolitic – 6.45% Dendritic – 0.6%</b>	<b>Yes – 9% No – 91%</b>
<b>Stromatolite B</b>	B3B-1	Quartz – 1% Calcite – 6% Micrite – 93%	Homogenous – 46.3% Peloidal – 37.6% Thrombolitic – 16.1% Dendritic – 0%	Yes – 29% No – 71%
	B3B-2	Quartz – 2% Calcite – 2% Micrite – 96%	Homogenous – 40.6% Peloidal – 30.2% Thrombolitic – 29.2% Dendritic – 0%	Yes – 5% No – 95%
	<b>Average (B)</b>	<b>Quartz – 1.5% Calcite – 4% Micrite – 94.5%</b>	<b>Homogenous – 43.45% Peloidal – 33.9% Thrombolitic – 22.65% Dendritic – 0%</b>	<b>Yes – 17% No – 83%</b>
<b>Stromatolite C</b>	C-4	Quartz – 16% Calcite – 17.5% Micrite – 66.5%	Homogenous – 40.6% Peloidal – 34.6% Thrombolitic – 24.8% Dendritic – 0%	Yes – 24.5% No – 75.5%
<b>AVERAGE</b>		<b>Quartz – 7.5% Calcite – 10.3% Micrite – 82.2%</b>	<b>Homogenous – 48.7% Peloidal – 33.2% Thrombolitic – 17.9% Dendritic – 0.2%</b>	<b>Yes – 16.8% No – 83.2%</b>

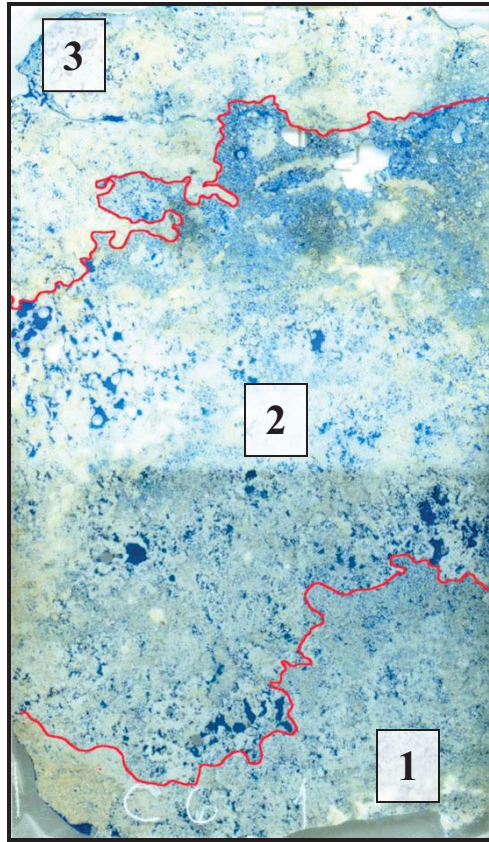


Figure 25 Thin section of a stromatolite depicting the three distinct zones



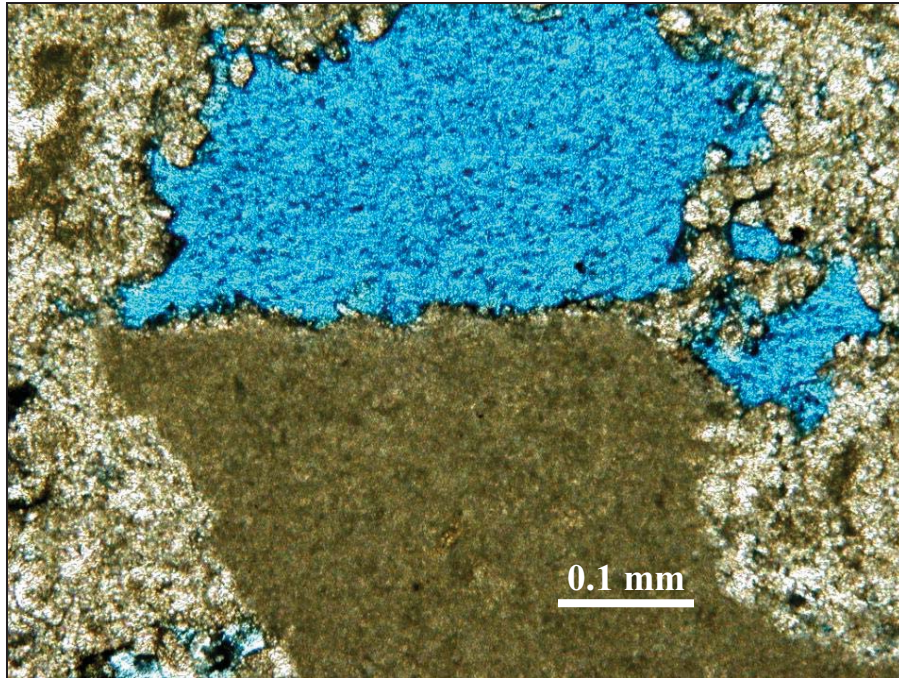


Figure 26 Geopetal structure within Zone 1 of a stromatolite sample (PPL)

### *Zone 2*

Zone 2 is darker in color compared to Zone 1 and Zone 3. Zone 2 contains more void spaces than the other two zones. The void spaces within Zone 2 are so substantial in some samples that a smooth surface is extremely difficult to produce with a table saw due to breakage of the sample. The structure within Zone 2 is very porous and is net-like in appearance (Fig. 27). Zone 2 contains the least amount of sediment than the other zones and is the most fragile when cut due to the ample amount of void space.





Figure 27 A porous Zone 2 within a stromatolite sample

### *Zone 3*

Zone 3 closely resembles Zone 1. Zone 3 is the most micritic of all three zones. Its color is almost as pure as the chalky white colors of Zone 1. Zone 3 exhibits the best examples of growth bands and is distinctly banded in some samples (Fig. 28). Zone 3 contains the least amount of void space and also includes ostracode carapaces incorporated into the micritic cortex as Zone 1. Zone 3 is the most consolidated and well-cemented zone of all three zones.



Figure 28 Distinct growth bands (indicated by arrows) within Zone 3 of a stromatolite sample

### Scanning Electron Microscopy Results

Stromatolite samples analyzed using the FESEM displayed globular surface textures resembling a surface coated by organically-induced microbial sludge (Fig. 29). On the surface of some examples, the same filamentous and/or fossilized microbial remnants observed by scanning electron microscopy in the ooid samples were found in patches on the stromatolite samples (Fig. 30). Bacteria-shaped, rod-like microbial remnants in the stromatolite samples averaged 50 – 250 nm in length. Fossilized microbial mucilage was also found in strands within the stromatolite samples (Fig. 31). The mucilage ranges from 10 – 20  $\mu\text{m}$  in length. The stromatolite samples also exhibited areas of sparry calcite cement similar to those found in the ooid samples.

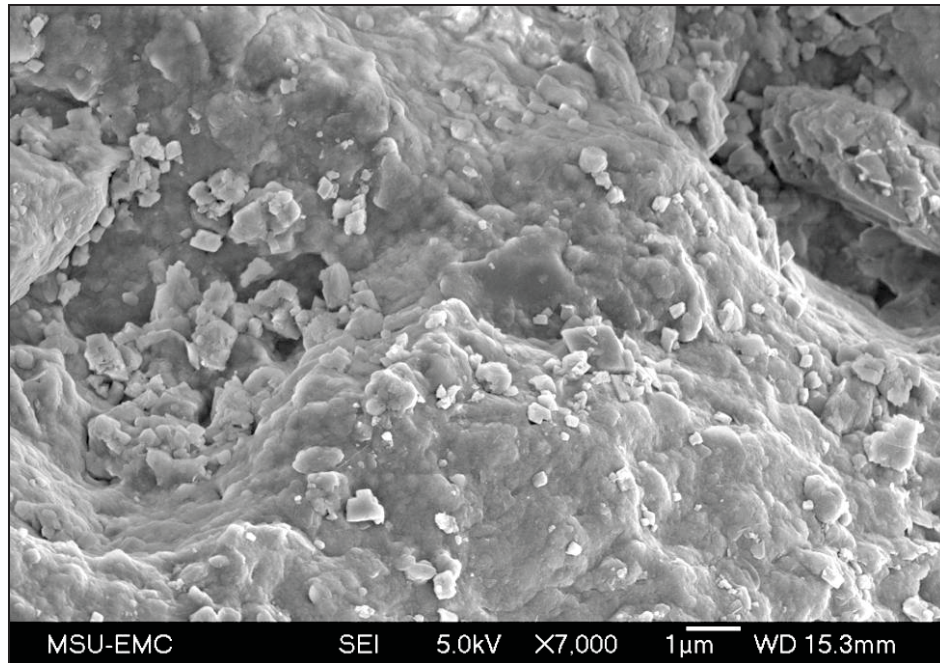


Figure 29 Globular textures dominate on broken stromatolite surface

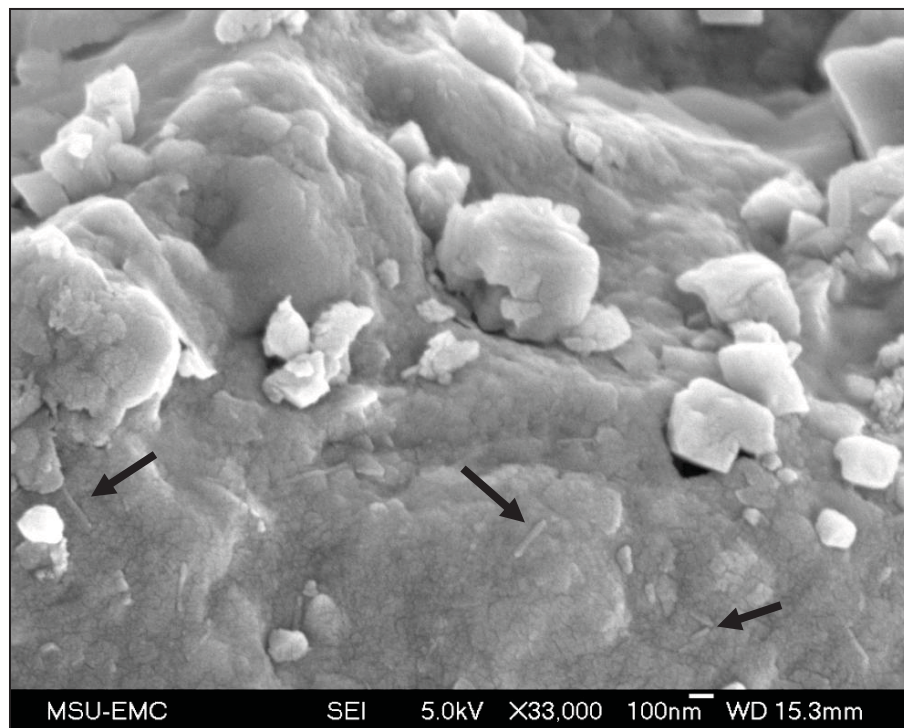


Figure 30 Rod-shaped bacteria (indicated by arrows) located on broken stromatolite surface



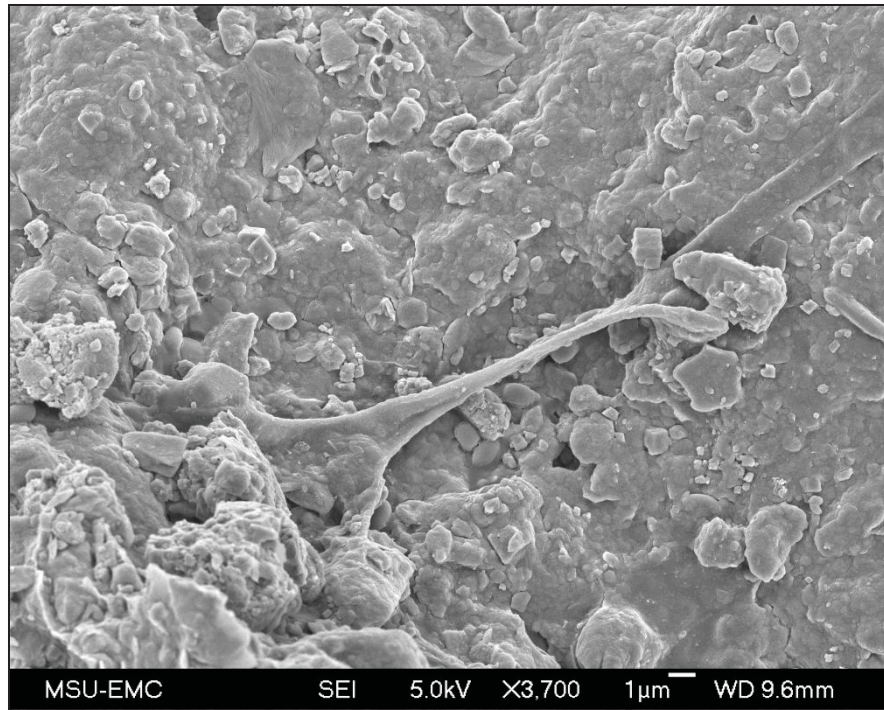


Figure 31 Fossilized microbial mucilage found in a stromatolite sample

## CHAPTER V

### DISCUSSION

#### **The Role of Organic Matter in the Channing Ooids**

Organic matter was found within the ooid samples in each layer (nucleus, micritic cortex, and cement) and was visible at both the microscopic level and by viewing with the SEM. Presence of organic matter varied from subtle to dominant, and their role ranged from deterioration of minerals to precipitation of calcium carbonate.

#### **Nucleus**

Ooid nuclei are presumed to be transported and weathered sediment originating from the Ogallala Formation. Evidence of pre-deposition microbial activity within the nuclei is ambiguous; however, microbial presence seems to favor feldspar nuclei over the quartz nuclei. Quartz nuclei exhibited no evidence of microbial presence whereas some feldspar nuclei distinctly appear to be experiencing microscale weathering (hydrolysis?) induced by an abundance of microbial filaments (Fig. 13).

#### **Micritic Cortex**

The micritic cortices are the most organic-rich zone within the ooids. The cortex consistently exhibited bulbous, globular textures which are unique to the involvement of

microbial processes during calcium carbonate precipitation. The unique mass of spheroids within the cortices are evidence of organic matter present at the time of precipitation. Microbial filaments and fossilized remnants covering the cortex were overwhelmingly abundant. The spheroidal texture of the cortex itself was frequently dominated by fossilized filaments (Fig. 12).

Organic matter dominates the ooid cortex and appears to be inextricable from its formation. The organic matter contains components similar to modern-day biofilms, filaments, mucilage and spheroidal textures. Likely “sticky” in nature, the cortex would have accumulated fine particles which were present in the water. Ostracode carapaces would have had a large, relatively flat surface to attach to the outer surface of the ooid. The sticky cortex coating allowed the incorporation of these ostracode carapaces. The sticky cortex also may have provided a microenvironment which likely enhanced calcium carbonate precipitation of micrite.

## **Cement**

The ooids were meteorically cemented by crystals of sparry calcite. SEM viewing revealed a majority of the calcite crystals faces exhibited both smooth and irregular textures within a single crystal (Fig. 16). Smooth crystal faces are produced by chemically-controlled processes; therefore the presence of irregular textures on crystal faces would imply the presence of an additional component to create the abnormality. Irregular crystal faces within carbonate crystals are attributed to the presence of organic matter at the time of mineral precipitation. The presence of irregular crystal faces contributes evidence in support of the study hypotheses and suggests that organic matter

was present when the mineral precipitated or that the mineral precipitated around the organic matter.

The sparry calcite cement appears to be an ordinary cement under low magnification ranges (10X – 20,000X); however, when viewed at higher magnifications (~40,000 – 130,000X), a few calcite cement crystals are sporadically covered in bacteria-shaped forms (Fig. 17). The average size of these forms was approximately 200 nm; however some measured ~800 nm. It is not suggested that forms are specifically bacterial in origin; however, the rod-shaped forms are interpreted as bacteria and the spheroidal forms may be nannobacteria or simply organic matter.

### **The Role of Organic Matter in the Channing Stromatolites**

The most distinct feature of the Channing Lake Basin stromatolites were the three zones visible in hand sample and thin section. Zoning within the stromatolites indicates environmental variations and overall change. The similarities between Zones 1 and 3 allow for the suggestion of similar lake conditions during the separate precipitation of these zones. Zones 1 and 3 also represent ideal conditions of calcium carbonate precipitation within the stromatolite. The presence of homogenous and peloidal micrites in successive growth bands indicate balance and order within the stromatolite. Zone 2 indicates a period in which the lake environment was changed by any matter of disturbances which could alter pH levels, salinity levels, or the water level of the lake.

SEM viewing of the stromatolite samples confirmed organic matter was prevalent in the form of fossilized filaments and microbial remnants (Fig. 30, Fig. 31). The smooth-flowing, conforming surface appearance of the stromatolites uncannily resembled

the texture of the micritic cortex in the ooid layer. Calcite crystals within the stromatolite samples also displayed smooth and irregular faces within single crystals, indicating organic presences at the time of precipitation. The presence of chemically-produced calcite crystals contiguous with the organically-produced smooth surface indicates a collaborative effort to produce the stromatolite.

### **Environment**

The environment in which the Channing Lake Basin ooids and stromatolites formed is suggested to be a lacustrine environment relatively high in alkalinity (Anderson and Kirkland, 1969). Abundant ostracodes and cyanophytes possibly indicate restrictive environmental conditions. The biota is of low diversity consisting of high tolerance organisms, further suggesting a stressed environment. Environmental indicators include *Limnocythere* sp. carapaces incorporated into the ooids and stromatolites, as well as distinct zoning within the stromatolites indicating a history of environmental variations, likely deepening to shallowing water conditions. Stromatolite zoning in collaboration with incorporated biota have allowed for the plausible suggestion that the zones in the stromatolites were formed within a lacustrine alkaline environment.

### **Ostracodes**

The ostracodes found within the ooid and stromatolite samples were previously determined to be *Limnocythere* sp. by Dr. Richard Benson (Personal Communication, Appendix B). *Limnocythere* sp. prefer lacustrine habitats and are frequently found in relatively calm waters as opposed to other species that dwell in running waters. In the



Rita Blanca lake bed varves, located below the ooid and stromatolite layers, three types of ostracodes were previously identified and are listed in order of abundance:

*Limnocythere sp.*, *Candona sp.*, and *Cyprideis sp.* (Benson, 1969). Mentioning ostracode species from lower strata is not meant to insinuate these are the species present within the ooid and stromatolite layers, but only as a reference as to what is possible.

### **Stromatolite Zoning**

Zones within the stromatolites are synonymous with their environment of deposition. Similar environments will produce similar layers. Color, texture, and porosity were the main components that varied between stromatolite zones. Zone 1 and 3 shared several characteristics such as color, micrite type (mainly homogenous and peloidal), lack of excessive porosity, and areas of abundant ostracodes. Zone 2 differed from Zones 1 and 3 in every aspect. The existence of zones within the stromatolite marks the change from one environment to another; therefore Zones 1 and 3 were very similar in environment with Zone 2 experiencing environmental stresses, probably deepening of the water level, and perhaps a chemical change in the water chemistry to a lower alkalinity.

### **Abiotic vs. Organic Origins**

Over the past century, the origin of stromatolites has been highly debated with the general consensus reversing several times. Ideas have included stromatolite formation as purely abiotic (Grotzinger and Rothman, 1996), as well as exclusively organic such as biomineralization (Riding, 2005). The Channing lake bed samples have overwhelmingly

provided data to support that a combination of chemical and organic processes are contributing factors to the precipitation of calcium carbonate.

## CHAPTER VI

### CONCLUSIONS

The research performed within this project has resulted in three main conclusions regarding the micritic ooids and stromatolites of the Channing Lake Basin.

The Channing ooids began as siliciclastic grains coated by an organic-rich micritic cortex into which ostracode carapaces were naturally incorporated. Meteoric cement also displays evidence of organic influences during precipitation.

Based on the ostracode species and zone alternations within the stromatolite samples, the stromatolites were formed within an evolving, varying lacustrine environment producing distinguishable zones.

A combination of organic and chemical processes resulted in calcium carbonate precipitation within the micritic ooids and stromatolites of Channing Lake Basin.

## REFERENCES

- [1] Aguirre, E. and G. Pasini. The Pliocene-Pleistocene Boundary. *Episodes*, vol. 8, pp. 116 – 120. 1985.
- [2] “Anadarko Basin.”  
<<http://www.nzlegacy.com/NZ%20Oil%20and%20Gas%20LLC.htm>>.  
New Mexico and Arizona Land Company, LLC. 19 April 2009
- [3] Anderson, Roger Y., and Douglas W. Kirkland. Paleocology of an Early Pleistocene Lake on the High Plains of Texas. *The Geological Society of America, Memoir 113*. Boulder, Colorado. 1969.
- [4] Benson, Richard H. Ostracodes of the Rita Blanca Lake Deposits. Smithsonian Institution. Washington, D. C. 1969.
- [5] Brown, C. N. The origin of caliche on the northeastern Llano Estacado, Texas: *Journal of Geology*, v. 64, no. 1, pp. 1-15; 1956.
- [6] “Channing, Texas: History.”  
<<http://www.texasescapes.com/TexasPanhandleTowns/Channing-Texas.htm>>.  
6 April 2009.
- [7] “Channing, Texas: Population.” United States Census Bureau.  
<[http://www.census.gov/popest/archives/2000s/vintage\\_2002/SUB-EST2002/SUB-EST2002-08-48.pdf](http://www.census.gov/popest/archives/2000s/vintage_2002/SUB-EST2002/SUB-EST2002-08-48.pdf)>. 10 April 2009.
- [8] Cummins, W. F. Report on the geography, topography, and geology of the Llano Estacado or Staked Plains. In: Dumble, E. T. (ed.). *Third Annual Report of the Geological Survey of Texas*, pp. 129 – 223. 1891.
- [9] Evans, G. L., and John P. Brand. Guidebook for 1956 Springfield Trip: Eastern Llano Estacado and adjoining Osage Plains – April 6-7, 1956. West Texas Geological Society and Lubbock Geological Society, 1 pg. 1956.
- [10] Evans, G. L., and G. E. Meade. Quaternary of the Texas High Plains. University of Texas Publication 4401, pp. 485-507. 1945.

- [11] Field Emission Scanning Electron Microscope Specifications at Mississippi State University. <<http://emcenter.msstate.edu>>. 10 April 2009.
- [12] Folk, Robert L. Detection of organic matter in thin sections of carbonate rocks using a white card. *Sedimentary Geology*, v. 54, issue 3, pp. 193 – 200. November 1987.
- [13] Folk, Robert. L. and F. Leo Lynch. The possible role of nannobacteria (dwarf bacteria) in clay-mineral diagenesis and the importance of careful sample preparation in high magnification SEM study. *Journal of Sedimentary Research*, v. 67, no. 3, pp. 583-589; May 1997.
- [14] Folk, Robert L. and F. Leo Lynch. Organic matter, putative nannobacteria, and the formation of ooids and hardgrounds. *Sedimentology*, v. 48, pp. 215-229. 2001.
- [15] Frye, J. C., and Leonard, A. B. Studies of Cenozoic geology along eastern margin of Texas High Plains, Armstrong to Howard counties. *University of Texas, Bureau of Economic Geology*, Investment Report 32, pp. 1 – 62. 1957.
- [16] Grotzinger, J. P., and D. H. Rothman. An abiotic model for stromatolite morphogenesis. *Nature*, v. 383, pp. 423 – 425.
- [17] Kirkland, Brenda L. Personal Communication.
- [18] Kirkland, Douglas W. Personal Communication. March 12, April 8, April 19, 2009.
- [19] Majewsky, O. P. Recognition of Invertebrate Fossil Fragments in Rocks and Thin Sections. Brill; Leiden.
- [20] Middleton, Gerard V., et al. Encyclopedia of Sediments and Sedimentary Rocks. Springer Reference Publishing. 2003. 928 pgs.
- [21] Milliken, Kitty, and Colin North. “The Editor’s Page.” *Journal of Sedimentary Research*, v. 75, pp. iii – iv. 2005.
- [22] Riding, Robert, et al. Calcareous Algae and Stromatolites. Springer-Verlag. Berlin, Heidelberg, Germany. 1991.
- [23] Riding, Robert, and L. Liang. Seawater chemistry control of marine limestone accumulation over the past 550 million years. *Revista Española de Micropaleontologica*, v. 37, no. 1, pp. 1 -11. 2005.
- [24] Warren, J. K. Evaporites: Sediments, Resources, and Hydrocarbons, p. 11, p. 263. Springer-Verlag. Berlin, Germany. 2006.

- [25] Whiteside, J. H. Arboreal stromatolites: a 210-million year record. *In*: Lowman, M. D. and B. Rinker (eds.). Forest Canopies (Physiological Ecology Series), 2<sup>nd</sup> edition, pp. 147-149. Academic Press. 2004.

APPENDIX A  
FIGURES AND TABLES CITED

## Figures Cited

- Figure 1. Location of Study Area. Drs. Richard J. Moiola and Douglas W. Kirkland. 1973.
- Figure 2. Measured section of the Rita Blanca Lake deposits. Drs. Richard J. Moiola and Douglas W. Kirkland. 1973.
- Figure 3. Oolite layer superimposing stromatolite layer. Dr. Brenda L. Kirkland. 1993.
- Figure 4. Cenozoic Stratigraphy of the Southern High Plains (Modified from Frye and Leonard, 1957b, and Evans, 1945). 1973.
- Figure 5. Stromatolite A. Personal photograph (digital scan). 25 September 2008.
- Figure 6. Stromatolite B. Personal photograph (digital scan). 25 September 2008.
- Figure 7. Field Emission Scanning Electron Microscope at the Electron Microscope Center, Mississippi State University, Mississippi State, MS.  
<<http://emcenter.msstate.edu>>. 10 April 2009.
- Figure 8. Hand sample of ooid layer. Personal Photograph (digital). 08 April 2009.
- Figure 9. Digital scan of smooth cut sample from the ooid layer. Personal Photograph (digital). 25 February 2010.
- Figure 10. Ostracode carapace incorporated within micritic coating (PPL).  
Dr. Douglas W. Kirkland. 1973.
- Figure 11. Nucleus, micritic cortex, and cement zones within an ooid. SEM image (digital). MSU-EMC. 01 October 2009.
- Figure 12. Filamentous microbial remnants within the micritic cortex of an ooid sample. SEM image (digital). MSU-EMC. 01 October 2009.
- Figure 13. Representative ooid nucleus (weathering feldspar). SEM image (digital). MSU-EMC. 03 September 2009.
- Figure 14. Boundary between micritic cortex and quartz nucleus. SEM image (digital). MSU-EMC. 01 October 2009.
- Figure 15. Example of sparry calcite cement in ooid layer. SEM image (digital). MSU-EMC. 03 September 2009.



- Figure 16. Examples of smooth and irregular crystal faces within a single sparry calcite crystal in ooid cement. SEM image (digital). MSU-EMC. 08 October 2009.
- Figure 17. High magnification image of bacteria-shaped bodies found on an irregular crystal face of a calcite crystal in ooid cement. SEM image (digital). MSU-EMC. 08 October 2009.
- Figure 18. Stromatolite hand sample with three zones indicated. Personal Photograph (digital scan). 25 September 2008.
- Figure 19. Upper surface of a stromatolite exhibiting a darker surface color compared to others. Personal Photograph (digital). 10 November 2009.
- Figure 20. Sample exhibiting abundant void spaces distributed within the middle section of a cut stromatolite sample. Personal photograph (digital scan). 25 September 2008.
- Figure 21. Example of homogenous/smooth micrite (PPL). Photomicrograph (digital). 9 February 2010.
- Figure 22. Example of peloidal micrite 20X (PPL). Photomicrograph (digital). 9 February 2010.
- Figure 23. Example of thrombotic/clotty micrite 20X (PPL). Photomicrograph (digital). 9 February 2010.
- Figure 24. Example of dendritic micrite 20X (PPL). Photomicrograph (digital). 9 February 2010.
- Figure 25. Thin section of a stromatolite depicting the three distinct zones. Personal photograph (digital scan). 08 April 2009.
- Figure 26. Geopetal structure within Zone 1 of a stromatolite sample (PPL). Personal photograph (digital). 09 February 2010.
- Figure 27. A porous Zone 2 within a stromatolite sample. Personal photograph (digital scan). 25 September 2008.
- Figure 28. Distinct growth bands within Zone 3 of a stromatolite sample. Personal photograph (digital scan). 25 September 2008.
- Figure 29. Globular textures dominate on a broken stromatolite surface. SEM image (digital). MSU-EMC. 01 October 2009.

Figure 30. Rod-shaped bacteria located on a broken stromatolite surface. SEM image (digital). MSU-EMC. 01 October 2009.

Figure 31. Fossilized microbial mucilage found in a stromatolite sample. SEM image (digital). MSU-EMC. 06 November 2008.

### **Tables Cited**

Table 1. Point Count Results on Ooid Layer Thin Sections. 13 October 2009.

Table 2. Point Count Results on Stromatolite Layer Thin Sections. 22 February 2010.

APPENDIX B  
PERSONAL COMMUNICATIONS

### **Personal Communications**

- [1] Dr. Richard Benson and Dr. Douglas W. Kirkland. "Ostracode Species Determination." January 5, 1968.
- [2] Dr. J. B. Thomas and Dr. Richard J. Moiola. "Oolite Samples to be compared with Jacka Samples". August 20, 1969.

SMITHSONIAN INSTITUTION  
UNITED STATES NATIONAL MUSEUM  
WASHINGTON, D. C. 20560

January 5, 1968

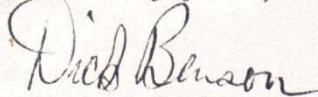
Dr. Douglas W. Kirkland  
Research Department  
Mobile Oil Corporation  
P.O. Box 900  
Dallas, Texas 75221

Dear Dr. Kirkland:

I have examined the photographs you sent to me on December 15th. The ostracodes which are represented in the oolitic sandstone seem to be of two types. You have several sections and photographs of one which has a depression in either side. This is a species of Limnocythere. I believe that this is a reasonably certain identification as there is only one other kind of fresh-water ostracode with such an outline. I failed to find it in the Rita Blanca fossil locality. You have seven photographs of this form and I have marked them with pencil on the back. Except one, the other photographs are probably cyprids. I would guess that they are Candona from the thinness of the wall and the general shape but this is uncertain. I could not confirm this from evidence in the pictures. The one photograph which you have marked "570 microns" is a section or a spore--oogonia. I would judge the ecology of these ostracodes would be the same as those of the Rita Blanca formation, when they were living. They may have been transported, but show no breakage.

The photographs are quite good. You were fortunate to get ones which contained enough of the outline for identification. I hope that these will be of some help to you.

Sincerely yours,



Richard H. Benson  
Curator, S.I.  
Professor of Geology  
University of Kansas

Enclosures



873 880 (8-67)

**INTEROFFICE CORRESPONDENCE**  
**MOBIL RESEARCH AND DEVELOPMENT CORPORATION**  
**Field Research Laboratory**

DATE August 20, 1969

TO R. J. Moiola

C. C.

OOLITE SAMPLES TO BE COMPARED WITH  
 JACKA SAMPLES

The following are general observations in crossed nicols and luminescence.

Sample T-2-W

Crossed Nicols

- 1) Basal, non-hematitic portion shows fine and very fine angular quartz and feldspar (perthite and microcline) clasts in a very fine microspar or micrite.
- 2) Slide becomes medium to coarse in remainder of slide in a gradational trend upward from end labelled "b"; associated is improved rounding, especially in coarser grains.
- 3) Several pieces of polycrystalline quartz in coarser portion of slide; vein quartz in coarser portion, only.
- 4) Oolites and pisolites with quartz and feldspar centers are very common; some oolites have no centers due to replacement.
- 5) Evidence of 2 generations of calcite; 1- coating of clasts, 2- cementation by spar of the oolites.
- 6) Some porosity - perhaps enhanced by slide preparation.

Luminescence

- 1) Definitely greater abundance of feldspar (10% vs. 5%) in lower, finer-grained band of the slide.
- 2) Recrystallized bivalves serve as cores of many oolites - some are ostracodes and some are charophytes.
- 3) Some quartz (and one plagioclase grain) in the section described in 1) is constant green in luminescence.
- 4) Most of calcite throughout slide is orange luminescent. Only in one portion is a small amount of the pore-fill spar banded black and orange. Faint growth lines evident in the micrite of the oolites. The calcite crystals rimming the oolites may be non-luminescent or weakly luminescent. Possibly 3 calcite generations, as above but also two stages of spar generation.
- 5) Replacement of some of the quartz and feldspar grains is very evident.

Sample T-4-E

Crossed Nicols

- 1) Generally medium to coarse-grained subangular and subrounded clasts in centers of oolites.
- 2) Several good pieces of polycrystalline quartz (granitic and metaquartzite fragments according to Folk); also recrystallized variety associated with veining in igneous rocks.

- 3) Larger monocrystalline quartz grains generally show straight bubble trains crossing at various angles.
- 4) Very little feldspar.
- 5) Rutilated quartz is common; some with elongate mineral inclusions.
- 6) Strange larger crystals about micrite-microspar oolites look like calcite but rhombic crystal form.

#### Luminescence

- 1) Possibly  $\frac{1}{4}$  of the oolites containing two or more clasts.
- 2) Feldspar grains are K-feldspar and occasionally albite (1-2% of clasts); 3 grains with feldspar overgrowths.
- 3) Material coating centers is darker orange luminescent calcite which is rimmed by brighter orange spar; little banding.
- 4) Calcite crystals coating the oolites does not have the typical dog-tooth spar habit (as previous slide also showed).
- 5) Very slight evidence of bivalves as in T-2-W, definitely ostracodes.
- 6) Higher frequency of center-less oolites and oolites which appear to have centers of lime mud (contemporaneous, micrite).
- 7) No green quartz present.
- 8) Bubble trains are fractures which have been healed.
- 9) Polycrystalline quartz of source rock type; (i.e., no in situ fracturing).

#### Sample T-1-S-W

#### Crossed Nicols

- 1) Clast size is fine to medium; many grains are very irregular along edges due to calcite replacement.
- 2) Many bivalve fragments, much recrystallization evident; ostracodes.
- 3) Much of the quartz shows straight-line bubble trains.
- 4) Feldspar is about 5% of the clasts.
- 5) Density of the oolites is greater than previous slides; some slightly squashed.

#### Luminescence

- 1) Definitely no banding in luminescent micrite coating the clasts; no granularity is noted and may be finer than previous micrite in oolites of previous slides.
- 2) Irregular luminescent spar coating the oolites (some black, some bright orange).
- 3) In areas where high concentrations of fossils, there is some pore fill calcite which is non-luminescent and very fine grained (Probably precipitated by the biota and no Mn activator present).
- 4) Quartz occasionally is deep blue with non-luminescent fracture-filling quartz.



Sample T-2-WCrossed Nicols

- 1) Grain size is fine to medium with fine and very fine clasts of quartz feldspar.
- 2) Degree of replacement of clasts is high (at least partial replacement).
- 3) Calcite is very dark due to clay or organic content, banded.
- 4) Oolites are rounded but micrite coatings of clasts (i.e., oolites) are thin.
- 5) Metamorphic, polymodal polycrystalline quartz is present.
- 6) Feldspar twinning types - microcline, albite, pericline.

Luminescence

- 1) Banding is rather subtle in the oolites.
- 2) Growth bands occasionally evident in the spar coating the oolites but in a very irregular manner - generally non-luminescent.
- 3) Feldspar and quartz grains occasionally crushed; the quartz is occasionally rehealed.
- 4) A micritic matrix material is present randomly throughout the slide. Several oolites are incorporated into it and luminescence is a dirty orange.
- 5) A few bivalve fragments are present but most are very small and occasionally broken up.
- 6) Some purple-blue luminescence along fractures of a few quartz grains.

Note - Bivalves are always represented in luminescence as opaque lines in the growth position of the organism.

Sample T-3-NCrossed Nicols

- 1) Grain size is coarse for oolites with medium to fine for the clasts of quartz and feldspar.
- 2) Mineralogy as in previous slides but probably about 5-6% feldspar, especially plagioclase (albite and oligoclase).
- 3) Packing density of oolites about same as in previous slides.
- 4) Few grains of quartz not coated.
- 5) Quartz looks like it is highly etched and included with bubbles.

Luminescence

- 1) Oolites consistently banded usually with a thin, bright orange covering of the clast followed with a weaker orange band and gradationally becoming much brighter to the outer edge.

- 2) The spar cement is fine crystalline, luminescent and non-luminescent. It doesn't fill pore spaces entirely.
- 3) Occasional deep blue quartz.
- 4) Few bivalves as before, may be seen in either manner (lum. or plane light).

Comparison to the Jacka Slides - Calichification(?)

1. The fossil content in the Moiola slides is far greater than in any Jacka slide.
2. Pseudospar or microspar is seen as a final outer blanket in both cases but the grain size and crystal forms are different.
3. More quartz and feldspar clasts are present in the Moiola samples (by a factor of 2).
4. The luminescence character of the calcite in the Moiola samples is far more constant than in Jacka slides where much of the calcite is non-luminescent micrite.
5. In Jacka slides there is a great deal of the replacement calcite (replacing quartz) which is non-luminescent; in Moiola slides, it is entirely luminescent.

6. *What Jacka areas as calichification  
does not fit the literature well  
at all.*

*J. B. Thomas*  
J. B. Thomas

JBT:mb